

Original research

Tacrolimus-binding protein FKBP8 directs myosin light chain kinase-dependent barrier regulation and is a potential therapeutic target in Crohn's disease

Li Zuo ^{1,2,3} Wei-Ting Kuo ^{2,3,4} Feng Cao,^{3,5} Sandra D Chanez-Paredes ^{2,3} Daniel Zeve ^{6,7} Prabhath Mannam,⁶ Léa Jean-François,³ Anne Day,³ W Vallen Graham,⁸ Yan Y Sweat ^{2,3} Nitesh Shashikanth,^{2,3} David T Breault ^{6,7} Jerrold R Turner ^{2,3,8}

► Additional supplemental material is published online only. To view, please visit the journal online (<http://dx.doi.org/10.1136/gutjnl-2021-326534>).

For numbered affiliations see end of article.

Correspondence to

Dr Jerrold R Turner and Dr Li Zuo, Department of Pathology, Brigham and Women's Hospital, Boston, Massachusetts, USA; JRTURNER@BWH.HARVARD.EDU, lzuo@bwh.harvard.edu

LZ and W-TK contributed equally.

Received 11 November 2021
Accepted 11 April 2022



© Author(s) (or their employer(s)) 2022. No commercial re-use. See rights and permissions. Published by BMJ.

To cite: Zuo L, Kuo WT, Cao F, *et al.* *Gut* Epub ahead of print: [please include Day Month Year]. doi:10.1136/gutjnl-2021-326534

ABSTRACT

Objective Intestinal barrier loss is a Crohn's disease (CD) risk factor. This may be related to increased expression and enzymatic activation of myosin light chain kinase 1 (MLCK1), which increases intestinal paracellular permeability and correlates with CD severity. Moreover, preclinical studies have shown that MLCK1 recruitment to cell junctions is required for tumour necrosis factor (TNF)-induced barrier loss as well as experimental inflammatory bowel disease progression. We sought to define mechanisms of MLCK1 recruitment and to target this process pharmacologically.

Design Protein interactions between FK506 binding protein 8 (FKBP8) and MLCK1 were assessed in vitro. Transgenic and knockout intestinal epithelial cell lines, human intestinal organoids, and mice were used as preclinical models. Discoveries were validated in biopsies from patients with CD and control subjects.

Results MLCK1 interacted specifically with the tacrolimus-binding FKBP8 PPI domain. Knockout or dominant negative FKBP8 expression prevented TNF-induced MLCK1 recruitment and barrier loss in vitro. MLCK1-FKBP8 binding was blocked by tacrolimus, which reversed TNF-induced MLCK1-FKBP8 interactions, MLCK1 recruitment and barrier loss in vitro and in vivo. Biopsies of patient with CD demonstrated increased numbers of MLCK1-FKBP8 interactions at intercellular junctions relative to control subjects.

Conclusion Binding to FKBP8, which can be blocked by tacrolimus, is required for MLCK1 recruitment to intercellular junctions and downstream events leading to immune-mediated barrier loss. The observed increases in MLCK1 activity, MLCK1 localisation at cell junctions and perijunctional MLCK1-FKBP8 interactions in CD suggest that targeting this process may be therapeutic in human disease. These new insights into mechanisms of disease-associated barrier loss provide a critical foundation for therapeutic exploitation of FKBP8-MLCK1 interactions.

INTRODUCTION

The intestinal barrier protects the internal milieu from luminal materials, including the microbiome.^{1,2} This barrier is formed by epithelial cells and the intercellular tight junctions that create a selectively-permeable seal between adjacent cells.

Significance of this study

What is already known on this subject?

- ⇒ Myosin light chain kinase is a critical intermediate in inflammation-induced intestinal barrier loss.
- ⇒ Increased epithelial myosin light chain kinase expression and activity correlate with disease severity in Crohn's disease.
- ⇒ Inflammatory stimuli trigger recruitment of MLCK1 to intercellular junctions; inhibition of this recruitment is therapeutic in experimental inflammatory bowel disease.

What are the new findings?

- ⇒ The tacrolimus-binding protein FKBP8 is a specific MLCK1 binding partner that directs MLCK1 to intercellular junctions.
- ⇒ Tacrolimus blocks FKBP8 binding to MLCK1 and reverses inflammation-induced barrier loss.
- ⇒ MLCK1-FKBP8 interactions are increased by inflammatory stimuli in model systems and in biopsies of patients with Crohn's disease.

How might it impact clinical practice in the foreseeable future?

- ⇒ The MLCK1-FKBP8 interaction is a potential therapeutic target in immune-mediated enterocolitis.
- ⇒ Inhibitors of MLCK1-FKBP8 binding could provide a non-immunosuppressive approach to barrier restoration.

Reduced barrier function, or increased permeability, can be caused by tight junction regulation or epithelial damage.³⁻⁵ These two forms of barrier loss occur by distinct mechanisms and have vastly different consequences. In contrast to epithelial damage, which allows unrestricted flux of bacteria, macromolecules, ions and water, regulated increases in tight junction permeability are more limited in extent and are both size-selective and charge-selective.⁶

Intestinal permeability increases similar to those induced by cytokines are a risk factor for

development of inflammatory bowel disease (IBD) in healthy first-degree relatives of patients with Crohn's disease.^{7,8} Limited permeability increases can also be a marker of impending relapse from remission in patients with Crohn's disease.⁹ Small increases in intestinal permeability may, therefore, significantly impact human disease. These observations suggest that barrier-restoring agents may prevent disease pathogenesis in healthy individuals with increased risk of developing IBD and may sustain remission in patients with Crohn's disease.

Myosin light chain kinase (MLCK), a canonical tight junction regulator, phosphorylates myosin II regulatory light chain (MLC) within the perijunctional actomyosin ring.¹ This increases tight junction permeability to molecules with diameters up to ~ 100 Å.^{8,10} Previous work using enzymatic inhibitors or knockout mice has shown that MLCK activity is required for acute, tumour necrosis factor (TNF)-induced increases in tight junction permeability *in vitro* and *in vivo*.^{11,12} Further study has demonstrated that MLCK-mediated increases in permeability drive chronic experimental immune-mediated IBD and graft-versus-host disease.^{13–15} Enzymatic MLCK inhibitors cannot, however, be developed as therapeutic agents because their effects on smooth, cardiac and skeletal muscle MLCK would lead to arrhythmia, hypotension, paralysis, aperistalsis and death.^{16–18} Targeting MLCK in order to restore barrier function will, therefore, require alternative approaches.

TNF induces recruitment of MLCK1, one of two MLCK splice variants expressed in intestinal epithelial cells, to the perijunctional actomyosin ring.^{19,20} MLCK2, the other MLCK splice variant, is not recruited to the perijunctional actomyosin ring despite differing from MLCK1 by only a single 227 nucleotide exon that is uniquely present in MLCK1. This sequence completes an amino-terminal immunoglobulin-like domain, IgCAM3, that can be targeted with a small drug-like molecule.²⁰ We recently showed that this molecule could block TNF-induced MLCK1 recruitment to prevent TNF-induced MLC phosphorylation and barrier loss without inhibiting MLCK enzymatic activity. This approach was more effective than anti-TNF antibodies in attenuating experimental IBD severity.²⁰

We hypothesised that the small molecule blocked MLCK1 recruitment to the perijunctional actomyosin ring by interfering with IgCAM3 binding to another protein. To test this idea, we probed a human intestinal epithelial cDNA library to discover MLCK1-specific binding proteins. This identified FK506-binding protein FKBP8, also known as FKBP38, a protein that has been linked to autophagy, mitophagy and the unfolded protein response but has no established function in intestinal epithelial cells.^{21–24}

Our data show that MLCK1 binds directly to FKBP8 and that these interactions are essential for MLCK1 recruitment, MLC phosphorylation and TNF-induced barrier loss. Moreover, biopsies from patients with Crohn's disease demonstrate an increase in MLCK1-FKBP8 interactions relative to control subjects. We have, therefore, elucidated the molecular mechanism of MLCK1 recruitment and established FKBP8 as a therapeutic target for intestinal barrier restoration in inflammatory disorders.

METHODS

Mice and ARRIVE guidelines

All studies were performed according to protocols approved by the Institutional Animal Care and Use Committees of the Brigham and Women's Hospital and Boston Children's Hospital. C57BL/6J mice were purchased from Jackson labs.

Human tissues

Biopsies from patients with Crohn's disease were obtained from Brigham and Women's Hospital under IRB-approved protocols. Only well-oriented colon biopsies with excellent tissue preservation were used. Biopsies with extensive ulceration were excluded. Colon biopsies without abnormalities from age-matched and sex-matched healthy patients, for example those undergoing screening colonoscopies, were used as controls.

Statistics

All data are presented as mean \pm SD and are representative of at least three independent experiments. Statistical significance was determined as indicated in each figure legend.

Patient and public involvement

We did not directly include patient and public involvement in this study. Patients were not invited to comment on the study design and were not consulted to interpret the results. Patients were not invited to contribute to the writing or editing of this manuscript.

Further methodological details are included in the online supplemental materials.

RESULTS

Myosin light chain kinase 1 (MLCK1) interacts specifically with the chaperone protein FKBP8

Under basal conditions, MLCK1 is present within both the cytoplasm and at the perijunctional actomyosin ring of differentiated intestinal epithelial cells (figure 1A). Treatment with tumour necrosis factor (TNF) increases MLCK1 expression and also induces a 4.3 ± 0.5 -fold increase in the perijunctional fraction of total cellular MLCK1 and a 6.0 ± 0.4 -fold increase in perijunctional MLC phosphorylation (figure 1B). Thus, TNF-induced increases in MLC phosphorylation correlate with MLCK1 recruitment to the perijunctional actomyosin ring following TNF treatment.^{19,20}

Although MLCK1 and MLCK2 splice variants differ only by the presence of IgCAM3 within the amino-terminal half of MLCK1 (figure 1C), MLCK2 is not specifically recruited to the perijunctional actomyosin ring. Moreover, we have shown that a small molecule targeting IgCAM3 can prevent MLCK1 recruitment.²⁰ We therefore hypothesised that IgCAM3-mediated interactions are essential for TNF-induced MLCK1 recruitment and sought to discover proteins that regulate this process. We employed a yeast two-hybrid screen to probe a human intestinal epithelial cell cDNA library (prey) using MLCK1 and MLCK2 IgCAM2-5 domain constructs as bait. MLCK1, but not MLCK2, bait captured sequence within the peptidyl-prolyl cis/trans isomerase (PPI) domain of FK506-binding protein 8 (FKBP8, also referred to as FKBP38).

We used yeast two-hybrid assays to further explore the specificity of the FKBP8-MLCK1 interaction. Full-length FKBP8 or mutants lacking the amino-terminal glutamate (E) rich domain (ERD), the PPI domain, the three tetratricopeptide (TPR) domains or the transmembrane (TM) domain were used as prey and screened against MLCK1 or MLCK2 IgCAM1-4 bait. All FKBP8 constructs, with the exception of that lacking the PPI domain, interacted with MLCK1 (figure 1C). In contrast, no FKBP8 constructs interacted with MLCK2. Thus, MLCK1 interacts specifically with FKBP8 via interactions that require the MLCK1 IgCAM3 and FKBP8 PPI domains.

In contrast to MLCK1, neither expression nor distribution of FKBP8 was affected by TNF (figure 1D). To determine whether TNF modified MLCK1-FKBP8 interactions within intestinal epithelial cells, we performed a proximity ligation assay in

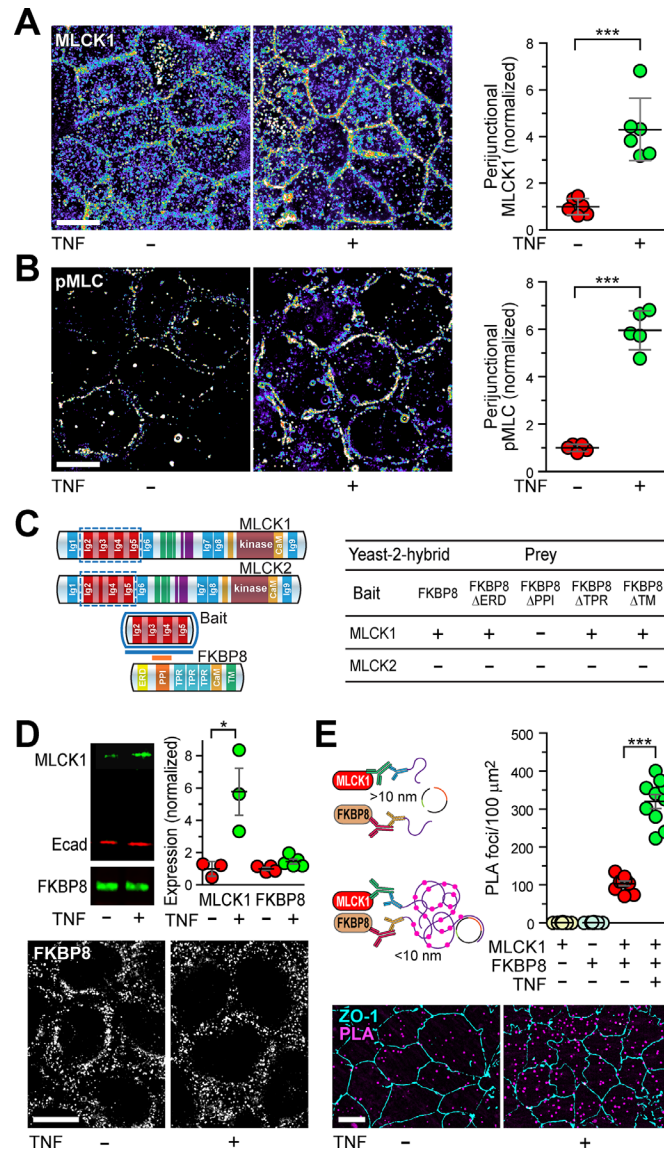


Figure 1 FKBP8 is an MLCK1-specific binding partner. (A,B) Caco-2 monolayers were treated with vehicle or TNF (1 ng/mL) for 4 hours, fixed and immunostained for MLCK1 (A) and pMLC (B). TNF increased total MLCK1 expression, the perijunctional MLCK1 fraction and perijunctional MLC phosphorylation. Pseudocolor intensity images are shown. Bar=10 μm. n=6 (A) or 5 (B) with each point representing an average of 3–5 fields within independent samples. These data are representative of >3 independent experiments. (C) Protein domain structure of the two *MYLK1* gene products, long MLCK1 and long MLCK2, expressed in intestinal epithelial cells. A region of MLCK1 or MLCK2 encompassing IgCAM2-5 was used as bait in a yeast two-hybrid screen of a human intestinal epithelial cDNA library. Sequence encoding the peptidyl-prolyl cis/trans isomerase (PPIase)/FK506-binding domain of FKBP8, a 413 amino acid member of the FK506 (tacrolimus) binding protein family, was recovered specifically with MLCK1 bait. Yeast two-hybrid assays using MLCK1 or MLCK2 IgCAM1-4 regions and 5 different FKBP8 constructs confirmed the MLCK1-specific interaction with the FKBP8 PPIase domain. (D) Western blots of vehicle and TNF-treated monolayers show that TNF induces MLCK1, but not FKBP8 expression. E-cadherin (Ecad) is shown as a loading control. Immunofluorescent staining failed to demonstrate any effect of TNF on FKBP8 distribution. (E) PLA using secondary antibodies conjugated to hybridising connector oligonucleotides allow the ligase to form a closed, circle DNA template that undergoes rolling-circle amplification if the connector oligonucleotides are within 10 nm of one another. Amplification is detected using a fluorescent-conjugated oligonucleotide probe (magenta). Negative controls omitted each primary antibody. ZO-1 (cyan) is shown for reference. Each point represents an average number of interaction sites detected within a single monolayer. n=5–10 independent monolayers for each condition, which are representative of >3 independent experiments. Bars=10 μm. *P<0.05; ***p<0.001; Student's t-test. MLC, myosin light chain; PLA, proximity ligation assay; pMLC, phosphorylated MLC.

which a positive signal is generated when MLCK1 and FKBP8 are within 10 nm of one another.²⁵ Small numbers of MLCK1-FKBP8 interaction sites were detected in untreated monolayers but these increased 3.1±0.1-fold following TNF stimulation (figure 1E). MLCK1 and FKBP8 interactions are, therefore, amplified in response to TNF-induced signalling events.

Direct MLCK1 binding to FKBP8 requires the PPI domain and can be inhibited by tacrolimus (FK506) and MLCK1 IgCAM3

The proximity ligation assay data indicate a close association between MLCK1 and FKBP8 but do not demonstrate a direct interaction between these two proteins. We used microscale thermophoresis to detect physical interactions between recombinant,

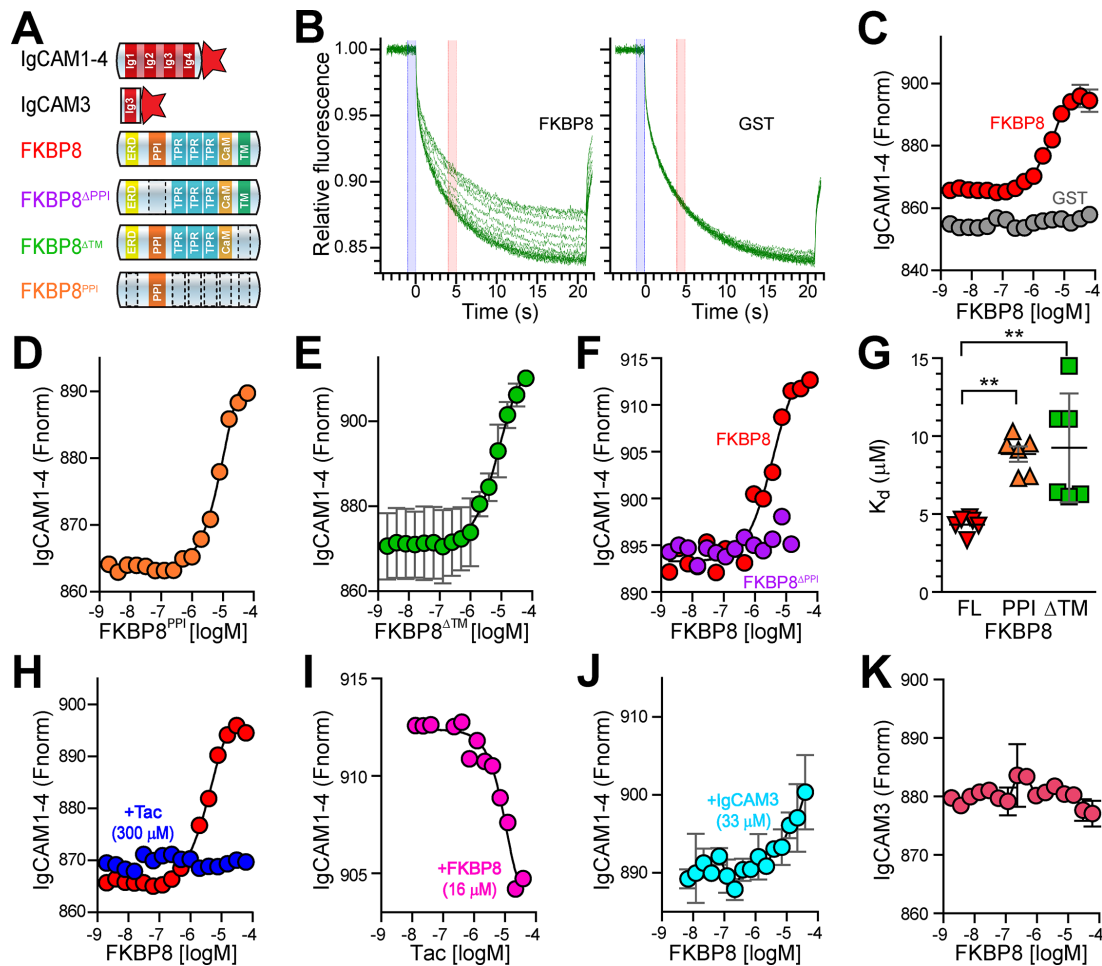


Figure 2 MLCK1 binds directly to the FKBP8 PPI domain. (A) Domain structures of MLCK1 and FKBP8 recombinant proteins used for MST. MLCK1 IgCAM1-4 was his-tagged (star). IgCAM3 was used as an unlabelled protein (J) or with a his tag (K). (B) Representative MST traces showing interactions of IgCAM1-4 with FKBP8 or, as a negative control, GST. (C–F) Dose-response binding curves of indicated unlabelled ligands with 10 nM labelled MLCK1 IgCAM1-4. (G) Dissociation constant (K_d) of FL, isolated PPI domain (PPI) or transmembrane domain deleted (Δ TM) FKBP8 with MLCK1 IgCAM1-4. $n=3-6$ independent assays and are representative of results using independent protein preparations. (H) MLCK1 IgCAM1-4 (10 nM) was mixed with tacrolimus (300 μ M) 10 min before assaying binding to FKBP8. (I) MLCK1 IgCAM1-4 (10 nM) and FKBP8 (16 μ M) were mixed and incubated for 10 min before adding tacrolimus at indicated concentrations. The IC_{50} of tacrolimus for the MLCK1-FKBP8 interaction is $69 \pm 13 \mu$ M. (J) Labelled MLCK1 IgCAM1-4 (10 nM) was mixed with unlabelled IgCAM3 (33 μ M) and incubated for 10 min before assaying binding to FKBP8. IgCAM3 blunted but did not completely block, MLCK1 IgCAM1-4 binding to FKBP8. (K) Direct binding of IgCAM3 to FKBP8 was not detected. ** $p < 0.01$; ANOVA with Bonferroni correction. ANOVA, analysis of variance; FL, full length; GST, glutathione-S-transferase; MST, microscale thermophoresis; PPI, peptidylprolyl isomerase.

fluorescent-tagged MLCK1 domains and untagged FKBP8 (figure 2A). Binding between IgCAM1-4 and FKBP8 was saturable and displayed first-order kinetics (figure 2B,C). Similarly, IgCAM1-4 bound directly to the FKBP8 PPI domain (figure 2D) and an FKBP8 mutant lacking the TM domain (figure 2E) but not PPI domain-deficient FKBP8 (figure 2F). Direct binding of MLCK1 IgCAM1-4 to FKBP8 therefore requires the PPI domain (figure 2F,G).

In addition to possessing the PPI enzymatic activity, the PPI domain is the site of tacrolimus (FK506) interactions with FK506-binding proteins. Consistent with this, tacrolimus completely blocked direct binding of MLCK1 IgCAM1-4 to FKBP8 (figure 2H) in a dose-dependent manner with an IC_{50} of $68.7 \pm 13.3 \mu$ M (figure 2I). MLCK1 IgCAM1-4 binding to FKBP8 was also inhibited by recombinant IgCAM3 (figure 2J), although a direct interaction between IgCAM3 and FKBP8 was too weak to be detected (figure 2K). Tacrolimus may,

therefore, inhibit intracellular interactions between MLCK1 and FKBP8.

Tacrolimus displaces MLCK1 from the perijunctional actomyosin ring, increases barrier function and reverses TNF-induced barrier loss

The binding data suggest that tacrolimus may be able to disrupt MLCK1 binding to FKBP8 in living cells and interfere with MLCK1 localisation at the perijunctional actomyosin ring. To assess this, MLCK1 localisation was assessed in Caco-2 monolayers after treatment with tacrolimus or, as a control, the enzymatic MLCK inhibitor PIK. Tacrolimus displaced MLCK1 from the perijunctional actomyosin ring, caused dose-dependent increases in transepithelial electrical resistance (TER) and reduced 3 kD dextran flux without affecting 70 kD dextran flux (online supplemental figure S1C, D). Tacrolimus therefore reduces flux across the leak pathway. PIK also reduced

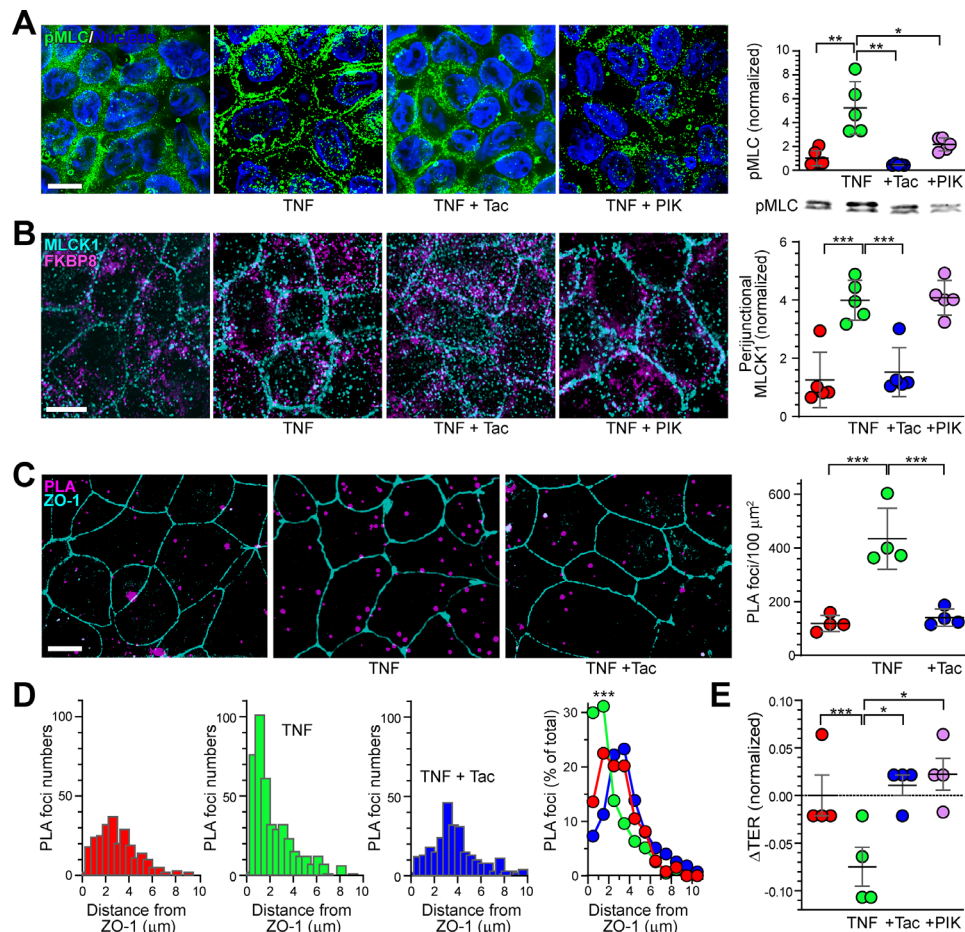


Figure 3 Tacrolimus reverses TNF-induced MLC phosphorylation, MLCK1 recruitment, MLCK1-FKBP8 interactions, and barrier loss. (A,B) Monolayers were treated with vehicle or TNF (1 ng/mL) for 4 hours, after which vehicle, tacrolimus (150 μ M) or PIK (200 μ M) were added apically. TER was measured and monolayers were fixed 0.5 hours later. Representative immunostains and quantitative morphometry of pMLC (green), MLCK1 (cyan) and FKBP8 (magenta) are shown. Nuclei (blue) are shown for reference in panel A. $n=5$ independent samples for each condition, which are representative of >3 independent experiments. Bar=10 μ m. (C) Proximity ligation assay (magenta) detecting interactions between MLCK1 and FKBP8. TNF increased and tacrolimus reduced the number of MLCK1-FKBP8 interactions. ZO-1 (cyan) is shown for reference. Data, $n=4$, are representative of >3 independent experiments with similar results. (D) The distance of each MLCK1-FKBP8 interaction site to the junction, defined as the nearest ZO-1 label, is shown. TNF-induced interactions (green) were close to the junction, while the few interactions detected before TNF treatment (red) are more diffusely distributed. Tacrolimus (blue) displaced TNF-induced interaction sites away from the junction. Gaussian fits are shown. (E) TNF reduced barrier function (TER). Tacrolimus (blue) and PIK (pink) were each able to reverse this barrier loss. Data, $n=4$, are representative of >3 independent experiments with similar results. * $P<0.05$; ** $p<0.01$; *** $p<0.001$; ANOVA with Bonferroni correction. ANOVA, analysis of variance; MLC, myosin light chain; pMLC, phosphorylated MLC.

paracellular permeability (online supplemental figure S1C) but did not affect MLCK1 localisation (online supplemental figure S1A, B).

We next asked if tacrolimus was able to reverse TNF-induced MLCK1 recruitment and MLC phosphorylation within the perijunctional actomyosin ring. Monolayers were treated with tacrolimus or PIK following TNF-induced barrier loss. Both tacrolimus and PIK reduced TNF-induced perijunctional MLC phosphorylation to levels similar to monolayers that were not treated with TNF (figure 3A, online supplemental figure S1E). However, only tacrolimus displaced MLCK1 from the perijunctional actomyosin ring (figure 3B). Moreover, tacrolimus reduced the number of MLCK1-FKBP8 interactions detected by proximity ligation assay (figure 3C). Analysis of the position of these proximity ligation assay-detectable interaction sites showed that they were distributed throughout the cell before TNF treatment but were closely associated with tight junctions, as marked by ZO-1, after TNF treatment (figure 3D). Tacrolimus both

reduced numbers of interaction sites and scattered the remaining sites throughout the cytoplasm (figure 3D). Consistent with this, tacrolimus reversed TNF-induced barrier loss as well as an enzymatic MLCK inhibitor (figure 3E). Tacrolimus did not, however, inhibit MLCK enzymatic activity (online supplemental figure S1F). Thus, TNF increased the number of MLCK1-FKBP8 interactions, in total and within 1–2 μ m of the tight junction, while tacrolimus disrupted and dispersed interaction sites. Pharmacological inhibition of MLCK1-FKBP8 interactions is, therefore, sufficient to reverse TNF-induced molecular events that lead to increased tight junction permeability.

FKBP8 deletion enhances epithelial barrier function and prevents TNF-induced barrier loss

The data obtained in living cells suggest that tacrolimus reverses TNF-induced barrier loss by preventing MLCK1-FKBP8 interactions. However, tacrolimus can affect many

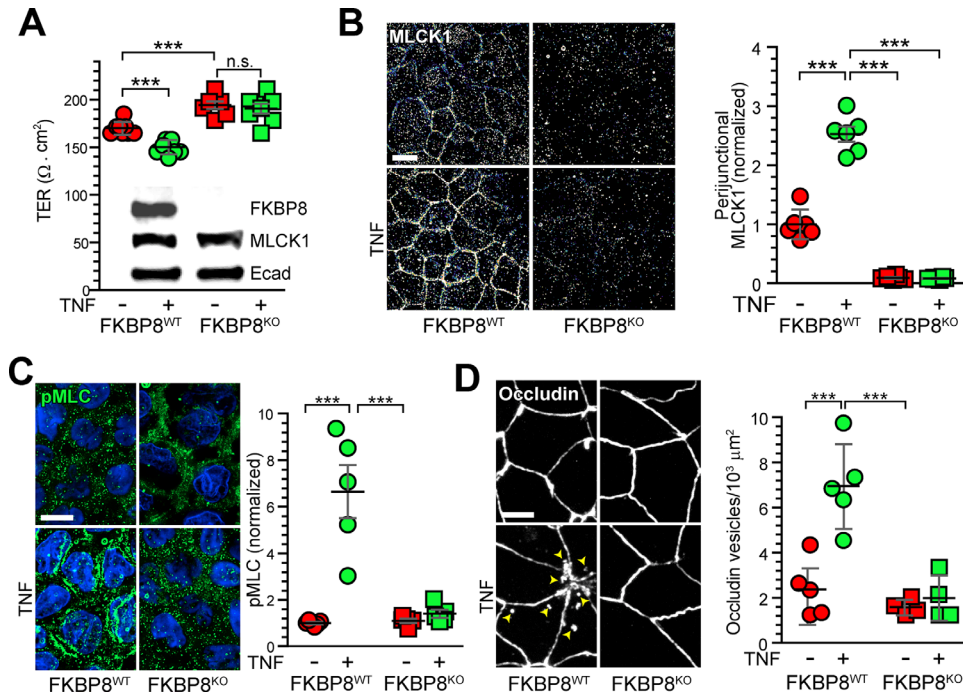


Figure 4 FKBP8 KO blocks TNF-induced MLCK1 recruitment, MLC phosphorylation, occludin internalisation and barrier loss. (A) Western blots confirm loss of FKBP8 expression in *FKBP8* KO Caco-2 cells. MLCK1 expression was not affected by *FKBP8* deletion. E-cadherin (Ecad) is shown as a loading control. Basal TER of *FKBP8*^{KO} monolayers was increased, relative to WT and was unaffected after 4-hour TNF treatment. Data, *n*=8, are representative of three independent experiments with similar results. (B–D) MLCK1 localisation (B), pMLC (green) (C), and occludin endocytosis (D) were determined in WT and *FKBP8*^{KO} monolayers before and after 4-hour TNF treatment. Prior to TNF treatment, perijunctional MLCK1 content is markedly reduced in *FKBP8*^{KO} monolayers relative to WT. MLCK1 recruitment, MLC phosphorylation and occludin endocytosis were all unaffected by TNF in *FKBP8*^{KO} cells. Data, *n*=5, are representative of three independent experiments with similar results. ****P*<0.001; ANOVA with Bonferroni correction. ANOVA, analysis of variance; KO, knockout; MLC, myosin light chain; pMLC, phosphorylation MLC; WT, wild type.

processes, as it binds to other proteins and inhibits calcineurin.^{26,27} To more specifically define its functional contributions, we knocked out *FKBP8* in intestinal epithelial cells (online supplemental figure S2A,B). This caused a modest increase in claudin-1 transcription but did not affect expression of claudin-1 protein or other tight junction proteins (online supplemental figure S2C–F).

TER of *FKBP8*^{KO} monolayers was 14%±6% higher than that of FKBP8-expressing monolayers (figure 4A). This coincided with a dramatic loss of junction-associated MLCK1 (figure 4B) despite normal overall MLCK1 expression (figure 4A, online supplemental figure S2E,G). FKBP8-deficient monolayers were completely protected from TNF-induced barrier loss (figure 4A), perijunctional MLCK1 recruitment (figure 4B), MLC phosphorylation (figure 4C) and occludin endocytosis (figure 4D). This was not due to defective TNF signalling, as both NFκB and p38 MAPK signalling pathways were activated normally in *FKBP8*^{KO} cells (online supplemental figure S2H–J). Thus, FKBP8 is a key regulator of barrier function and is essential to perijunctional MLCK1 localisation at steady-state as well as TNF-induced MLCK1 recruitment and barrier loss.

FKBP8 acts as a scaffolding protein that regulates the epithelial barrier and mediates TNF-induced MLCK1 perijunctional recruitment

Although two independent *FKBP8*^{KO} Caco-2 cell clones behaved similarly, we sought to exclude the possibility of CRISPR-induced off-target genomic changes or clonal variation as explanations for the functional deficits induced by FKBP8 knockout. To this end, we generated stably

transfected *FKBP8*^{KO} Caco-2 cells with inducible mCherry-FKBP8 expression (figure 5A). Induction of mCherry-FKBP8 expression in *FKBP8*^{KO} monolayers reduced TER to levels indistinguishable from those of parental Caco-2 monolayers (figure 5B). The increase in permeability that resulted from mCherry-FKBP8 expression was reversed by tacrolimus (figure 5C). In contrast, tacrolimus had no effect on TER of *FKBP8*^{KO} monolayers without mCherry-FKBP8 expression. mCherry-FKBP8 expression corrected steady-state MLCK1 localisation at the perijunctional actomyosin ring (figure 5D). Moreover, *FKBP8*^{KO} monolayers expressing mCherry-FKBP8 displayed TNF-induced MLCK1 recruitment and barrier loss (figure 5D,E). FKBP8 therefore directs both basal and TNF-induced MLCK1 recruitment and associated barrier regulation.

FKBP8 is a multidomain scaffold that binds to many proteins, including microtubule-associated protein 1A/1B-light chain 3 (LC3), prolyl hydroxylase domain protein 2 and heat-shock protein 90β(HSP90β). We, therefore, hypothesised that FKBP8 might link MLCK1 to another protein involved in perijunctional recruitment (figure 5F). To test this hypothesis, we expressed either the free PPI domain (FKBP8^{PPI}) or a FKBP8 deletion mutant lacking the PPI domain (FKBP8^{ΔPPI}), reasoning that, if FKBP8 does link another protein to MLCK1, these should act as dominant negative inhibitors of TNF-induced MLCK1 recruitment and barrier loss (figure 5F). Consistent with this hypothesis, inducible expression of FKBP8^{PPI} in monolayers of cells expressing endogenous full-length FKBP8 increased TER and blunted TNF-induced MLCK1 recruitment (figure 5G,H). Similarly, FKBP8^{ΔPPI} expression reduced perijunctional MLCK1

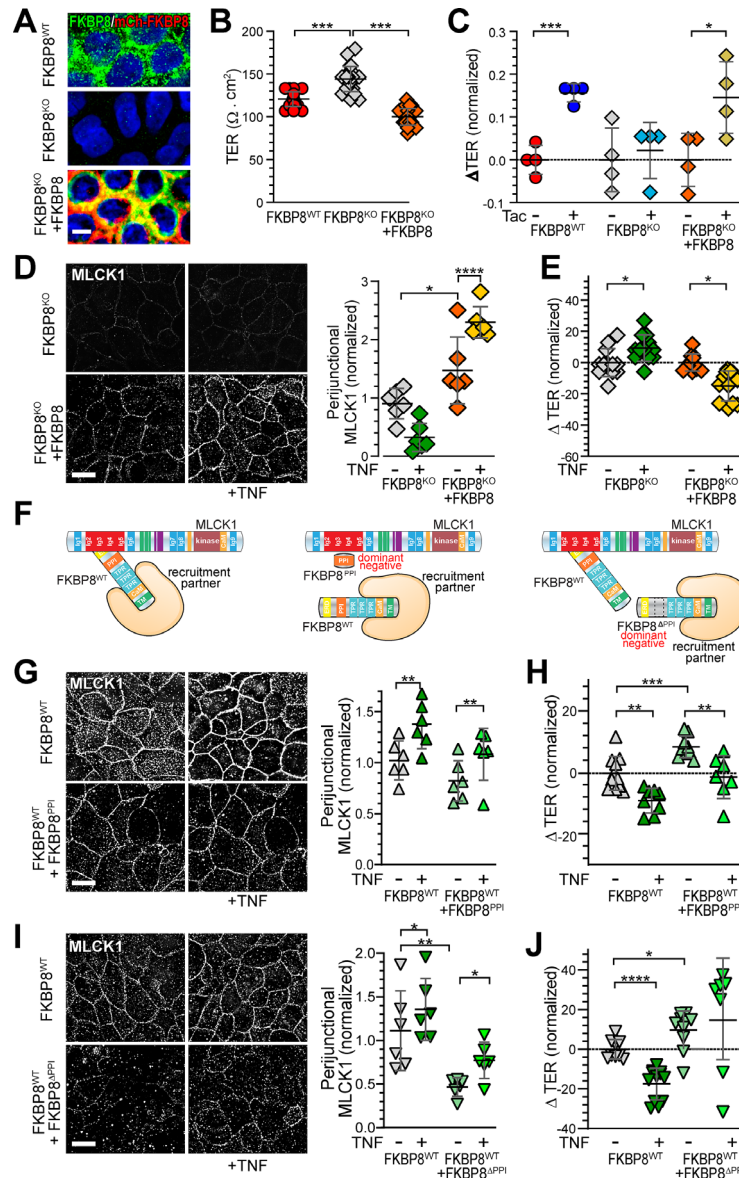


Figure 5 FKBP8 mutants are dominant negative effectors that block MLCK1 recruitment. (A) *FKBP8*^{KO} cells were stably transfected to express mCherry-FKBP8 from an inducible promoter. Fluorescence micrographs show WT Caco-2 and transfected *FKBP8*^{KO} Caco-2 without (KO) or with (+FKBP8) induction of mCherry-FKBP8 (red). Both mCherry-tagged and endogenous FKBP8 were detected by immunostain (green). Nuclei (white) are shown for reference. Bar=10 μm. (B) Steady-state TER of *FKBP8* KO is greater than WT. mCherry-FKBP8 expression (+FKBP8) reduces TER to values comparable to WT. Data (n=24) are representative of >5 independent experiments with similar results. (C) TER of WT, KO and *FKBP8*^{KO} with mCherry-FKBP8 expression (+FKBP8) monolayers was measured 2 hours after apical addition of vehicle or tacrolimus (150 μM). Tacrolimus increased TER of WT and +FKBP8 monolayers but had no effect on KO monolayers. Data (n=4) are representative of >4 independent experiments with similar results. (D,E) TNF treatment for 4-hours TNF triggered MLCK1 recruitment (D) and barrier loss (E) in +FKBP8, but not KO, monolayers. Data (n=8) are representative of >4 independent experiments with similar results. (F) Proposed model by which FKBP8 links MLCK1 to an unidentified recruitment partner (*left*). Excess free PPI domain occupies MLCK1 binding sites, thereby acting as a dominant negative effector by preventing endogenous FKBP8 from linking MLCK1 to the recruitment partner (*middle*). Excess *FKBP8*^{ΔPPI} expression occupies binding sites on the recruitment partner, thereby acting as a dominant negative effector that prevents endogenous FKBP8 from linking MLCK1 to the recruitment partner (*right*). (G,H) Induction of free PPI domain (*FKBP8*^{PPI}) expression in WT cells limits both TNF-induced MLCK1 recruitment (32% vs 23% increase in perijunctional MLCK1 in non-induced vs induced cells, respectively) and TER loss. Data (n=6–8) are representative of >3 independent experiments with similar results. (I,J) Induction of *FKBP8*^{ΔPPI} expression in WT cells limits TNF-induced MLCK1 recruitment (58% vs 23% increase in perijunctional MLCK1 in non-induced vs induced cells, respectively) and prevents TNF-induced TER loss. Data (n=6–8) are representative of >3 independent experiments with similar results. For all graphs, each point represents an individual monolayer. For morphological data, each point is an average of multiple microscopic fields analysed with an individual monolayer. *P<0.05; **p<0.01; ***p<0.001; ANOVA with Bonferroni correction. ANOVA, analysis of variance; KO, knockout; PPI, peptidylprolyl isomerase; WT, wild type.

localisation, both before and after TNF treatment, increased basal TER, and prevented TNF-induced barrier loss (figure 5I,J). Thus, although we have not identified the interacting partner,

these data strongly suggest that a region other than the PPI domain allows FKBP8 to link MLCK1 to another component of the molecular machinery that directs perijunctional recruitment.

Tacrolimus prevents TNF-induced perijunctional MLCK1 recruitment, MLC phosphorylation and FKBP8 interactions in human organoids

Although Caco-2 cell monolayers are an established model in which the initial discoveries that long MLCK, specifically MLCK1, mediates TNF-induced barrier loss were made,^{11 20 28 29} these are transformed cells and may not always faithfully recapitulate responses of non-transformed epithelium. Organoids offer an alternative to Caco-2,³⁰ but, despite expression of differentiation markers, these models often fail to display differentiated function. A recently reported approach to in vitro differentiation of human small intestinal epithelial stem cells grown in 3D matrix³¹ substantially increased expression of differentiation markers *SGLT1*, *ALP1* and *MUC2* while reducing expression of the stem cell marker *LGR5* (online supplemental figure S3). More importantly, TNF increased MLCK1 expression in these cells within 4 hours (figure 6A), similar to the effects and kinetics previously reported in vitro using Caco-2 monolayers,^{29 32} in vivo using acute mouse models^{13 32 33} and ex vivo using human intestinal biopsies.²⁰ TNF also induced MLCK1 recruitment to the perijunctional actomyosin ring, MLC phosphorylation and MLCK1 association with FKBP8, as measured by proximity ligation assay (figure 6B–D). Addition of tacrolimus 4 hours after TNF treatment began reversed MLCK1 recruitment, MLC phosphorylation and FKBP8 association (figure 6B–D). Thus, human intestinal epithelial stem cell organoid cultures recapitulate the results obtained using Caco-2 cells, thereby demonstrating that the effect is not an artefact of transformation and validating Caco-2 cells as a model of TNF-induced, FKBP8-mediated MLCK1 recruitment.

Tacrolimus prevents T cell activation-induced perijunctional MLCK1 recruitment, MLC phosphorylation and barrier loss in vivo

Tacrolimus is a potent inhibitor of T cell activation that has been used as a systemic immunosuppressive agent in transplantation and IBD. It would, therefore, be impossible to differentiate tacrolimus effects on MLCK1 recruitment and immune activation in chronic disease models. As an alternative, we asked if local tacrolimus delivery could prevent acute cytokine-induced MLCK1 recruitment, MLC phosphorylation and barrier loss in vivo independent of generalised immunosuppression. A segment of jejunum was functionally isolated and lumenally perfused beginning 1 hour after systemic T cell activation (figure 7A).^{12 20 34} Mucosal TNF, IFN γ and IL1 β content and intraepithelial T cell numbers were all increased by 3 hours after T cell activation (figure 7B,C). These mucosal responses to systemic T cell activation were unaffected by inclusion of tacrolimus within the perfusate (figure 7B,C). Moreover, tacrolimus did not interfere with cytokine-induced transcriptional activation of *Mylk1*,^{32 35} which encodes epithelial MLCK1 (figure 7D).^{19 36} Lumenally delivered tacrolimus is, therefore, insufficient to inhibit mucosal immune activation or anti-CD3 induced TNF signalling in immune and epithelial cells.

Despite intact T cell and cytokine responses, luminal tacrolimus blocked perijunctional MLCK1 recruitment, MLC phosphorylation and occludin internalisation (figure 7E–G). This indicates that, as shown in vitro, FKBP8 is essential for MLCK1 recruitment in vivo. Moreover, tacrolimus blocked anti-CD3-induced increases in lumen-to-serum 4 kD dextran flux (figure 7H). Importantly, neither anti-CD3 nor tacrolimus affected lumen-to-serum flux of 70 kD dextran, thereby demonstrating that epithelial damage is not involved in either acute T cell activation-induced permeability increases or tacrolimus-mediated inhibition of this response (online

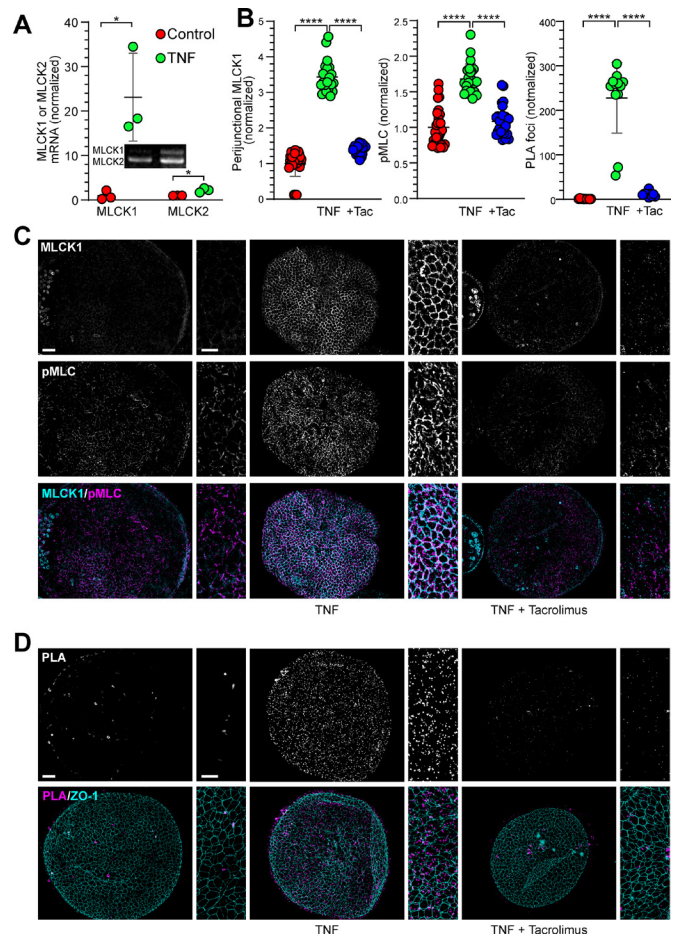


Figure 6 Tacrolimus prevents TNF-induced perijunctional MLCK1 recruitment, MLC phosphorylation and FKBP8 interactions in human organoids. (A) Differentiated human small intestinal organoids were grown in 3D and treated with 1 ng/mL TNF for 4 hours; MLCK1 and MLCK2 were detected by semiquantitative PCR.¹⁹ $n=3$. Student's t-test, $*p<0.05$. (B) Differentiated organoids were treated with vehicle or TNF (1 ng/mL) for 4 hours, after which vehicle, tacrolimus (150 μ M) or PIK (200 μ M) were added for 2 hours before fixation. Immunostains and proximity ligation assay were quantified morphometrically. $n=15-28$ organoids per condition in this representative experiment. (C) TNF-induced perijunctional MLCK1 (cyan) recruitment was blocked by tacrolimus. TNF-induced MLC phosphorylation (pMLC, magenta) was blocked by tacrolimus. (D) Representative images of proximity ligation assay detecting the interaction between MLCK1 and FKBP8 (magenta) in human organoids treated with TNF, tacrolimus. ZO-1 (cyan) is shown for reference. The number of MLCK1-FKBP8 interacting sites is markedly increased with TNF and reduced by tacrolimus. Bars=50 or 20 μ m (high magnification images). MLC, myosin light chain; pMLC, phosphorylation MLC.

supplemental figure S4). Specific anti-CD3-induced increases in leak pathway permeability and reversal by tacrolimus were confirmed by evaluating the ratio of 4 kD dextran to 70 kD dextran.^{3 37} Thus, by mechanisms independent of immunosuppression, tacrolimus prevents T cell activation-induced, MLCK1 recruitment and leak pathway barrier loss in vivo.

Crohn's disease is characterised by increased perijunctional MLCK1 recruitment and MLCK1-FKBP8 interaction

Finally, we sought to determine whether our observations using reductionist in vitro systems and a simple, acute in vivo

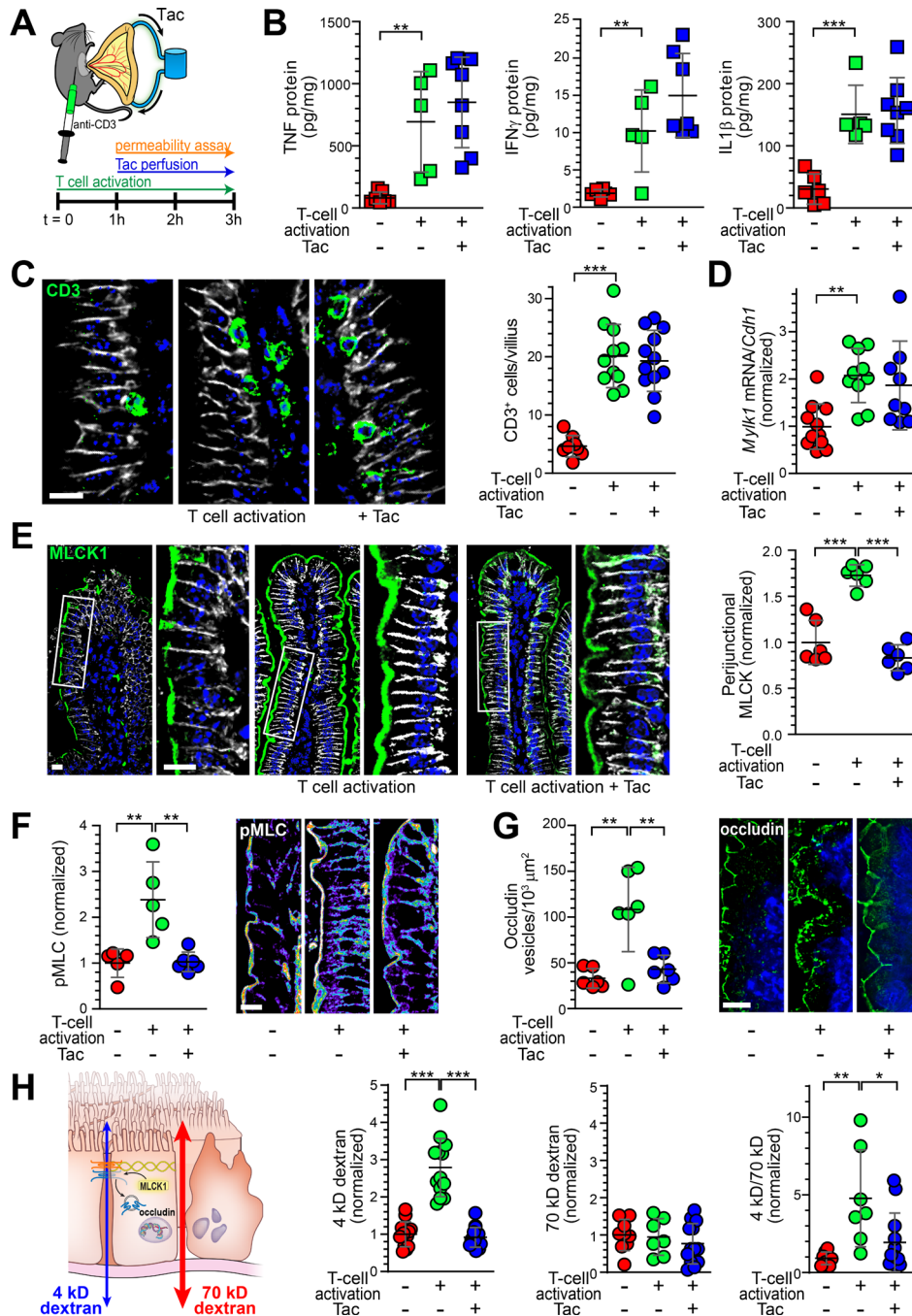


Figure 7 Tacrolimus prevents acute T cell activation-induced barrier dysfunction in vivo. **A.** Mice were injected with vehicle or anti-CD3 (200 μ g, i.p.). Jejunal loops were isolated without disrupting the neurovasculature. One hour after T cell activation, the lumen was perfused with a saline and glucose solution containing vehicle or tacrolimus (300 μ M) as well as 4 kD and 70 kD dextrans. Serum and tissues were harvested after 2 hours of perfusion (3 hours after T cell activation). **(B)** ELISA shows that mucosal TNF, IFN γ and IL1 β were all increased after T cell activation. This was not inhibited by luminal perfusion with tacrolimus. Data ($n=5-6$) are representative of three independent experiments with similar results. **(C)** Tacrolimus did not prevent increases in jejunal intraepithelial T cells (green) after anti-CD3 injection. Na⁺-K⁺ ATPase (white) and nuclei (blue) are shown for reference. Bar=10 μ m. Data ($n=7-10$) are representative of 3 independent experiments with similar results. **(D)** T cell activation-induced transcription of *Mylk*, which encodes epithelial MLCK1, was not affected by tacrolimus. Data ($n=7-10$) are representative of 3 independent experiments with similar results. **(E)** T cell activation-induced perijunctional MLCK1 (green) recruitment was blocked by tacrolimus. Na⁺-K⁺ ATPase (white) and nuclei (blue) are shown for reference. Bars=20 μ m. **(F)** T cell activation-induced pMLC (pseudocolor) was blocked by tacrolimus. Bar=10 μ m. **(G)** T cell activation-induced occludin (green) endocytosis was blocked by tacrolimus. Nuclei (blue) are shown for reference. Bar=10 μ m. Data ($n=6$) shown in E-G are representative of three independent experiments. **(H.)** The tight junction leak pathway, which is regulated by MLCK1, accommodates 4 kD, but not 70 kD, dextran. Epithelial damage increases flux of both 4 kD and 70 kD dextrans across the unrestricted pathway. T cell activation selectively upregulates the leak pathway, as indicated by increases in both 4 kD dextran flux and 4 kD/70 kD permeability ratio without any change in 70 kD dextran flux. Tacrolimus restored leak pathway barrier function. The absence of increased 70 kD dextran flux excludes epithelial damage as a mechanism of 4 kD dextran flux. $n=7-13$. * $P<0.05$; ** $p<0.01$; *** $p<0.001$; ANOVA with Bonferroni correction; MLC, myosin light chain; pMLC, phosphorylation MLC.

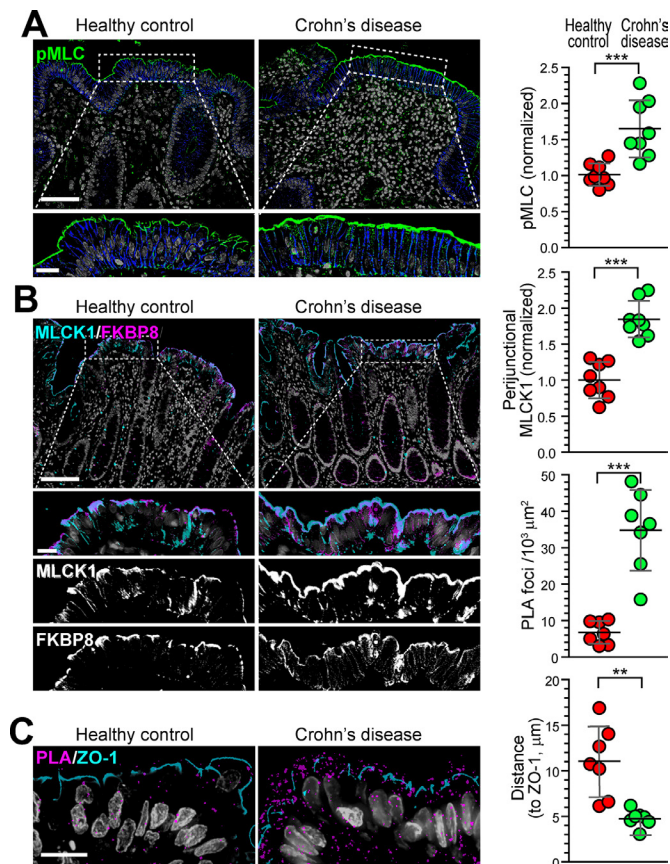


Figure 8 Perijunctional MLCK1 recruitment and MLCK1-FKBP8 interactions are increased in Crohn's disease. (A) Representative immunofluorescence of phosphorylated MLC (pMLC, green) in colon biopsies from patients with Crohn's disease (4 male; 4 female; average age 32 ± 9 years) and age-matched and sex-matched healthy control subjects (4 male; 4 female; average age 36 ± 10 years). $\text{Na}^+\text{-K}^+\text{-ATPase}$ (blue) and nuclei (grey) are shown for reference. Bars = $10 \mu\text{m}$. Quantitative morphometry shows significantly greater perijunctional phosphorylated MLC in Crohn's disease. $n=8$ patients and eight controls. (B) Representative immunofluorescence of MLCK1 (cyan) and FKBP8 (magenta) in colon biopsies from patients with Crohn's disease and healthy control subjects. Nuclei (grey) are shown for reference. Bars = $10 \mu\text{m}$. Perijunctional MLCK1 is significantly increased in biopsies of patient with Crohn's disease relative to healthy control subject biopsies. $n=8$ patients and eight controls. (C) Representative images of proximity ligation assay detecting interactions between MLCK1 and FKBP8 (magenta) in biopsies from patients with Crohn's disease and healthy control subjects. ZO-1 (cyan) and nuclei (grey) are shown for reference. The number of MLCK1-FKBP8 interaction sites is markedly increased and the distance of these sites from the tight junction is reduced in Crohn's disease biopsies relative to healthy control subject biopsies. $n=7$ patients and 7 controls. For all graphs, each point represents the mean of multiple measurements of a single biopsy from an individual patient or healthy subject. $**P < 0.01$; $***p < 0.001$; Student's t-test. MLC, myosin light chain; pMLC, phosphorylation MLC.

model were relevant to the pathobiology of Crohn's disease. We evaluated ileal biopsies from patients with Crohn's disease and age-matched and sex-matched healthy controls undergoing surveillance colonoscopy. Consistent with our previous report,³⁸ MLC phosphorylation and perijunctional MLCK1 were both increased in biopsies of patient with Crohn's disease (figure 8A,B). In contrast, expression and distribution of FKBP8

were similar in Crohn's disease and healthy control biopsies. We then used the proximity ligation assay to assess in vivo MLCK1-FKBP8 interactions. The number of interaction sites was ~ 5 -fold greater in Crohn's disease biopsies relative to healthy controls (figure 8C). These sites were concentrated with $1\text{-}2 \mu\text{m}$ of the tight junction (figure 8C). Crohn's disease is therefore associated with marked increases in both perijunctional MLCK1 localisation and perijunctional MLCK1-FKBP8 interactions. These data support the conclusion that the MLCK1-FKBP8 interactions drive perijunctional MLCK1 recruitment in Crohn's disease.

DISCUSSION

MLCK is a key regulator of tight junction permeability in disease.^{1 13 14 20} Studies using genetically modified mice and enzymatic inhibitors have demonstrated that MLCK inhibition prevents acute, cytokine-induced diarrhoea and attenuates chronic, immune-mediated experimental IBD.^{12 13 39} MLCK is, therefore, a promising therapeutic target. It is not, however, possible to target MLCK enzymatic activity, as this is essential to organ function and cell behaviour. We recently discovered an alternative approach using a small molecule that blocks MLCK-mediated barrier regulation by preventing recruitment of the MLCK1 splice variant of intestinal epithelial MLCK to the perijunctional actomyosin ring without affecting enzymatic activity.^{19 20} In vitro, this small molecule was as effective as an enzymatic inhibitor that abolished MLCK1 kinase activity without blocking recruitment.²⁰ In vivo, drug-induced displacement of MLCK1 from the perijunctional actomyosin ring was more effective than anti-TNF antibodies in experimental IBD.²⁰ Agents that inhibit MLCK1 recruitment may, therefore, be viable as pharmacological therapies that safely restore the intestinal epithelial barrier. We hypothesised that such agents would interfere with interactions between MLCK1 and other proteins that direct recruitment. Here, we used a yeast two-hybrid screen to identify FKBP8 as one such MLCK1 binding protein.

Recombinant protein analyses demonstrated that the unique IgCAM3 domain within MLCK1 interacts directly with the tacrolimus-binding PPI domain of FKBP8. Experiments using cultured monolayers in which FKBP8 was knocked out or FKBP8 mutants were expressed as dominant negative effectors showed that MLCK1-FKBP8 interactions are required for MLCK1 recruitment. Tacrolimus, which binds to the PPI domain, blocked FKBP8 binding to MLCK1 and prevented MLCK1 recruitment in TNF-treated human organoids as well as T cell activation-induced barrier loss in mice. Finally, analysis of patient biopsies established MLCK1 recruitment and increased numbers of MLCK1-FKBP8 interactions in Crohn's disease. Together, these data show that FKBP8 is a MLCK1-binding protein and an essential component of the molecular machinery that recruits MLCK1 to the perijunctional actomyosin ring.

FKBP8 is unusual among FKBP family proteins due to its presence at multiple intracellular sites and established roles as a chaperone and regulator of protein stability.^{22 40} The PPIase activity of FKBP8 promotes protein folding, likely explaining the ability of FKBP8 to attenuate the unfolded protein response.⁴¹ FKBP8 binds to a wide range of proteins, including LC3 (via a site within the ERD domain),²¹ cystic fibrosis TM conductance regulator (CFTR) via the PPI domain,²² Hsp90 β , the hepatitis C virus non-structural protein 5A and cullin-4 (via the TPR domains)⁴²⁻⁴⁴ and calmodulin.⁴⁵ Our data showing that either the PPI domain alone or FKBP8 ^{Δ PPI} have dominant negative effects indicate that, through the PPI and another domain, FKBP8 forms a scaffold that brings MLCK1 into a larger recruitment complex. Although

further study will be needed to clarify whether FKBP8-mediated MLCK1 recruitment requires only FKBP8 scaffolding function or also depends on PPIase activity. Notably, IgCAM3 includes five prolines that could be targets of the PPIase.

FKBP8^{KO} epithelial cells were used to demonstrate the essential contributions of FKBP8 to TNF-induced MLCK1 recruitment and tight junction barrier regulation. It would have been desirable to extend these studies using *Fkbp8* knockout mice, but, unfortunately, these suffer from embryonic lethality.⁴⁶ Instead, we used tacrolimus and an acute, TNF-dependent model of intestinal barrier loss following systemic T cell activation to assess FKBP8 function in vivo. Although tacrolimus is an immunosuppressive calcineurin inhibitor, we found that luminal delivery via direct perfusion did not affect anti-CD3-induced mucosal immune activation. Tacrolimus did, however, block T cell activation-induced MLCK1 recruitment, MLC phosphorylation and barrier loss. These data show that FKBP8-dependent recruitment is required for MLCK1-mediated tight junction barrier regulation in vivo. Moreover, the results suggest that mechanisms of tacrolimus action in IBD could include barrier regulation, although immunosuppression must be the dominant mechanism. Monofunctional FKBP inhibitors that do not inhibit calcineurin and are not immunosuppressive have been developed, including one that specifically targets FKBP8.⁴⁷ Although that molecule is not commercially available, we speculate that it or similar molecules might be effective non-immunosuppressive barrier restorative agents.

In summary, the data identify FKBP8 as an MLCK1-interacting protein that directs MLCK1 recruitment to the perijunctional actomyosin ring, demonstrate that this interaction is enhanced in experimental inflammatory models and human IBD and show that tacrolimus (FK506) blocks this interaction and corrects TNF-induced barrier loss in vitro and in vivo. This new insight into fundamental mechanisms of cytokine-induced barrier loss may form a foundation for future therapeutic exploitation of FKBP8-MLCK1 interactions.

Author affiliations

¹Anhui Medical University, Hefei, Anhui, China

²Department of Pathology, Harvard Medical School, Boston, Massachusetts, USA

³Laboratory of Mucosal Barrier Pathobiology, Department of Pathology, Brigham and Women's Hospital, Boston, Massachusetts, USA

⁴Graduate Institute of Oral Biology, National Taiwan University, Taipei, Taiwan

⁵Department of Otorhinolaryngology Head and Neck Surgery, Second People's Hospital of Hefei, Hefei, Anhui, China

⁶Pediatrics, Boston Children's Hospital, Boston, Massachusetts, USA

⁷Department of Pediatrics, Harvard Medical School, Boston, Massachusetts, USA

⁸Department of Pathology, The University of Chicago, Chicago, Illinois, USA

Acknowledgements We thank Dr. Kelly L. Arnett and the Harvard Center for Macromolecular Interactions for instruction and assistance with microscale thermophoresis experiments, Dr. Bin Bao for his and the Harvard Digestive Disease Center for assistance with cell sorting, Tiffany S Davanzo (Slaybaugh Studios) for her beautiful illustrations and Heather Marlatt (Nationwide Histology) for her outstanding histological services and tissue microarray development.

Contributors Conceptualisation: LZ, W-TK, WVG, JRT. Experimentation: LZ, W-TK, FC, SDC-P, WVG, JRT. Data analysis: LZ, W-TK, FC, SDC-P, DZ, WVG, JRT. Manuscript preparation and revision: LZ, WTK, FC, SCP, DZ, WVG, PM, LI-F, AD, YVS, NS, DB, JRT.

Funding This work was supported by the National Natural Science Foundation of China grants 82070548 (LZ) and 81800464 (LZ) and U.S. National Institutes of Health grants R01DK61931 (JRT), R01DK68271 (JRT) and P30DK034854 (the Harvard Digestive Disease Center).

Competing interests WVG is a founder, shareholder and employee of Thelium Therapeutics. JRT is a founder and shareholder of Thelium Therapeutics and has served as a consultant for Entrinsic, Immunic, and Kallyope.

Patient and public involvement Patients and/or the public were not involved in the design, or conduct, or reporting, or dissemination plans of this research.

Patient consent for publication Not applicable.

Provenance and peer review Not commissioned; externally peer reviewed.

Data availability statement Data are available on reasonable request. Data, analytic methods and study materials will be made available to academic investigators on reasonable request.

Supplemental material This content has been supplied by the author(s). It has not been vetted by BMJ Publishing Group Limited (BMJ) and may not have been peer-reviewed. Any opinions or recommendations discussed are solely those of the author(s) and are not endorsed by BMJ. BMJ disclaims all liability and responsibility arising from any reliance placed on the content. Where the content includes any translated material, BMJ does not warrant the accuracy and reliability of the translations (including but not limited to local regulations, clinical guidelines, terminology, drug names and drug dosages), and is not responsible for any error and/or omissions arising from translation and adaptation or otherwise.

ORCID iDs

Li Zuo <http://orcid.org/0000-0001-8606-3050>

Wei-Ting Kuo <http://orcid.org/0000-0002-1230-0014>

Sandra D Chanez-Paredes <http://orcid.org/0000-0002-5889-8576>

Daniel Zeve <http://orcid.org/0000-0002-4117-1282>

Yan Y Sweat <http://orcid.org/0000-0002-9903-8054>

David T Breault <http://orcid.org/0000-0002-0402-4857>

Jerrold R Turner <http://orcid.org/0000-0003-0627-9455>

REFERENCES

- Zuo L, Kuo W-T, Turner JR. Tight junctions as targets and effectors of mucosal immune homeostasis. *Cell Mol Gastroenterol Hepatol* 2020;10:327–40.
- Luissint A-C, Parkos CA, Nusrat A. Inflammation and the intestinal barrier: leukocyte-epithelial cell interactions, cell junction remodeling, and mucosal repair. *Gastroenterology* 2016;151:616–32.
- Chanez-Paredes SD, Abtahi S, Kuo W-T, et al. Differentiating between tight junction-dependent and tight junction-independent intestinal barrier loss in vivo. *Methods Mol Biol* 2021;2367:249–71.
- Capaldo CT, Nusrat A. Cytokine regulation of tight junctions. *Biochim Biophys Acta* 2009;1788:864–71.
- Anderson JM, Van Itallie CM. Physiology and function of the tight junction. *Cold Spring Harb Perspect Biol* 2009;1:a002584.
- Weber CR, Raleigh DR, Su L, et al. Epithelial myosin light chain kinase activation induces mucosal interleukin-13 expression to alter tight junction ion selectivity. *J Biol Chem* 2010;285:12037–46.
- Turpin W, Lee S-H, Raygoza Garay JA, et al. Increased intestinal permeability is associated with later development of Crohn's disease. *Gastroenterology* 2020;159:2092–100.
- Buhner S, Buning C, Genschel J, et al. Genetic basis for increased intestinal permeability in families with Crohn's disease: role of CARD15 3020insC mutation? *Gut* 2006;55:342–7.
- Wyatt J, Vogelsang H, Hübl W, et al. Intestinal permeability and the prediction of relapse in Crohn's disease. *Lancet* 1993;341:1437–9.
- Pongkorsakol P, Turner JR, Zuo L. Culture of intestinal epithelial cell monolayers and their use in multiplex macromolecular permeability assays for in vitro analysis of tight junction size selectivity. *Curr Protoc Immunol* 2020;131:e112.
- Zolotarevsky Y, Hecht G, Koutsouris A, et al. A membrane-permeant peptide that inhibits MLC kinase restores barrier function in in vitro models of intestinal disease. *Gastroenterology* 2002;123:163–72.
- Clayburgh DR, Barrett TA, Tang Y, et al. Epithelial myosin light chain kinase-dependent barrier dysfunction mediates T cell activation-induced diarrhea in vivo. *J Clin Invest* 2005;115:2702–15.
- Su L, Nalle SC, Shen L, et al. TNFR2 activates MLCK-dependent tight junction dysregulation to cause apoptosis-mediated barrier loss and experimental colitis. *Gastroenterology* 2013;145:407–15.
- Nalle SC, Zuo L, Ong MLDM, et al. Graft-Versus-Host disease propagation depends on increased intestinal epithelial tight junction permeability. *J Clin Invest* 2019;129:902–14.
- Nalle SC, Kwak HA, Edelblum KL, et al. Recipient NK cell inactivation and intestinal barrier loss are required for MHC-matched graft-versus-host disease. *Sci Transl Med* 2014;6:243ra87.
- He W-Q, Peng Y-J, Zhang W-C, et al. Myosin light chain kinase is central to smooth muscle contraction and required for gastrointestinal motility in mice. *Gastroenterology* 2008;135:610–20.
- Ding P, Huang J, Battiprolu PK, et al. Cardiac myosin light chain kinase is necessary for myosin regulatory light chain phosphorylation and cardiac performance in vivo. *J Biol Chem* 2010;285:40819–29.
- Hortemo KH, Aronsen JM, Lunde IG, et al. Exhausting treadmill running causes dephosphorylation of sMLC2 and reduced level of myofilament MLCK2 in slow twitch rat soleus muscle. *Physiol Rep* 2015;3. doi:10.14814/phy2.12285. [Epub ahead of print: 22 02 2015].

- 19 Clayburgh DR, Rosen S, Witkowski ED, *et al.* A differentiation-dependent splice variant of myosin light chain kinase, MLCK1, regulates epithelial tight junction permeability. *J Biol Chem* 2004;279:55506–13.
- 20 Graham WV, He W, Marchiando AM, *et al.* Intracellular MLCK1 diversion reverses barrier loss to restore mucosal homeostasis. *Nat Med* 2019;25:690–700.
- 21 Bhujabal Z, Birgisdottir Ása B, Sjøttem E, *et al.* Fkbp8 recruits LC3A to mediate Parkin-independent mitophagy. *EMBO Rep* 2017;18:947–61.
- 22 Hutt DM, Roth DM, Chalfant MA, *et al.* FK506 binding protein 8 peptidylprolyl isomerase activity manages a late stage of cystic fibrosis transmembrane conductance regulator (CFTR) folding and stability. *J Biol Chem* 2012;287:21914–25.
- 23 Okamoto T, Nishimura Y, Ichimura T, *et al.* Hepatitis C virus RNA replication is regulated by FKBP8 and Hsp90. *Embo J* 2006;25:5015–25.
- 24 Walker VE, Atanasiu R, Lam H, *et al.* Co-chaperone FKBP38 promotes HERG trafficking. *J Biol Chem* 2007;282:23509–16.
- 25 Leuchowius K-J, Weibrecht I, Söderberg O. In situ proximity ligation assay for microscopy and flow cytometry. *Curr Protoc Cytom* 2011;Chapter 9:Chapter 9:Unit 9 36.
- 26 Shirane M, Nakayama KI. Inherent calcineurin inhibitor FKBP38 targets Bcl-2 to mitochondria and inhibits apoptosis. *Nat Cell Biol* 2003;5:28–37.
- 27 Schreiber SL. Immunophilin-sensitive protein phosphatase action in cell signaling pathways. *Cell* 1992;70:365–8.
- 28 Ma TY, Boivin MA, Ye D, *et al.* Mechanism of TNF- α modulation of Caco-2 intestinal epithelial tight junction barrier: role of myosin light-chain kinase protein expression. *Am J Physiol Gastrointest Liver Physiol* 2005;288:G422–30.
- 29 Wang F, Graham WV, Wang Y, *et al.* Interferon- γ - and tumor necrosis factor- α synergize to induce intestinal epithelial barrier dysfunction by up-regulating myosin light chain kinase expression. *Am J Pathol* 2005;166:409–19.
- 30 Donowitz M, Turner JR, Verkman AS, *et al.* Current and potential future applications of human stem cell models in drug development. *J Clin Invest* 2020;130:3342–4.
- 31 Zeve D, Stas E, de Sousa Casal J, *et al.* Robust differentiation of human enteroendocrine cells from intestinal stem cells. *Nat Commun* 2022;13:261.
- 32 Graham WV, Wang F, Clayburgh DR, *et al.* Tumor necrosis factor-induced long myosin light chain kinase transcription is regulated by differentiation-dependent signaling events. Characterization of the human long myosin light chain kinase promoter. *J Biol Chem* 2006;281:26205–15.
- 33 Marchiando AM, Shen L, Graham WV, *et al.* Caveolin-1-dependent occludin endocytosis is required for TNF-induced tight junction regulation in vivo. *J Cell Biol* 2010;189:111–26.
- 34 Musch MW, Clarke LL, Mamah D, *et al.* T cell activation causes diarrhea by increasing intestinal permeability and inhibiting epithelial Na⁺/K⁺-ATPase. *J Clin Invest* 2002;110:1739–47.
- 35 Ye D, Ma I, Ma TY. Molecular mechanism of tumor necrosis factor- α modulation of intestinal epithelial tight junction barrier. *Am J Physiol Gastrointest Liver Physiol* 2006;290:G496–504.
- 36 Lazar V, Garcia JG. A single human myosin light chain kinase gene (MLCK; MYLK). *Genomics* 1999;57:256–67.
- 37 Tsai P-Y, Zhang B, He W-Q, *et al.* IL-22 upregulates epithelial claudin-2 to drive diarrhea and enteric pathogen clearance. *Cell Host Microbe* 2017;21:671–81.
- 38 Blair SA, Kane SV, Clayburgh DR, *et al.* Epithelial myosin light chain kinase expression and activity are upregulated in inflammatory bowel disease. *Lab Invest* 2006;86:191–201.
- 39 Su L, Shen L, Clayburgh DR, *et al.* Targeted epithelial tight junction dysfunction causes immune activation and contributes to development of experimental colitis. *Gastroenterology* 2009;136:551–63.
- 40 Nielsen JV, Mitchelmore C, Pedersen KM, *et al.* FKBP8: novel isoforms, genomic organization, and characterization of a forebrain promoter in transgenic mice. *Genomics* 2004;83:181–92.
- 41 Misaka T, Murakawa T, Nishida K, *et al.* FKBP8 protects the heart from hemodynamic stress by preventing the accumulation of misfolded proteins and endoplasmic reticulum-associated apoptosis in mice. *J Mol Cell Cardiol* 2018;114:93–104.
- 42 Blundell KLIM, Pal M, Roe SM, *et al.* The structure of FKBP38 in complex with the MEEVD tetrapeptide binding-motif of Hsp90. *PLoS One* 2017;12:e0173543.
- 43 Okamoto T, Omori H, Kaname Y, *et al.* A single-amino-acid mutation in hepatitis C virus NS5A disrupting FKBP8 interaction impairs viral replication. *J Virol* 2008;82:3480–9.
- 44 Tani J, Shimamoto S, Mori K, *et al.* Ca(2+)/S100 proteins regulate HCV virus NS5A-FKBP8/FKBP38 interaction and HCV virus RNA replication. *Liver Int* 2013;33:1008–18.
- 45 Edlich F, Weiwad M, Erdmann F, *et al.* Bcl-2 regulator FKBP38 is activated by Ca2+/calmodulin. *Embo J* 2005;24:2688–99.
- 46 Bulgakov OV, Eggenschwiler JT, Hong D-H, *et al.* FKBP8 is a negative regulator of mouse sonic hedgehog signaling in neural tissues. *Development* 2004;131:2149–59.
- 47 Edlich F, Weiwad M, Wildemann D, *et al.* The specific FKBP38 inhibitor N-(N',N'-dimethylcarboxamidomethyl)cycloheximide has potent neuroprotective and neurotrophic properties in brain ischemia. *J Biol Chem* 2006;281:14961–70.

Supplemental Materials

Zuo L, Kuo W, Cao F, et al. The tacrolimus-binding protein FKBP8 directs myosin light chain kinase-dependent barrier regulation and is a potential therapeutic target in Crohn's disease. Gut 2022. doi: [gutjnl-2021-326534](https://doi.org/10.1136/gutjnl-2021-326534)

Supplemental Figures

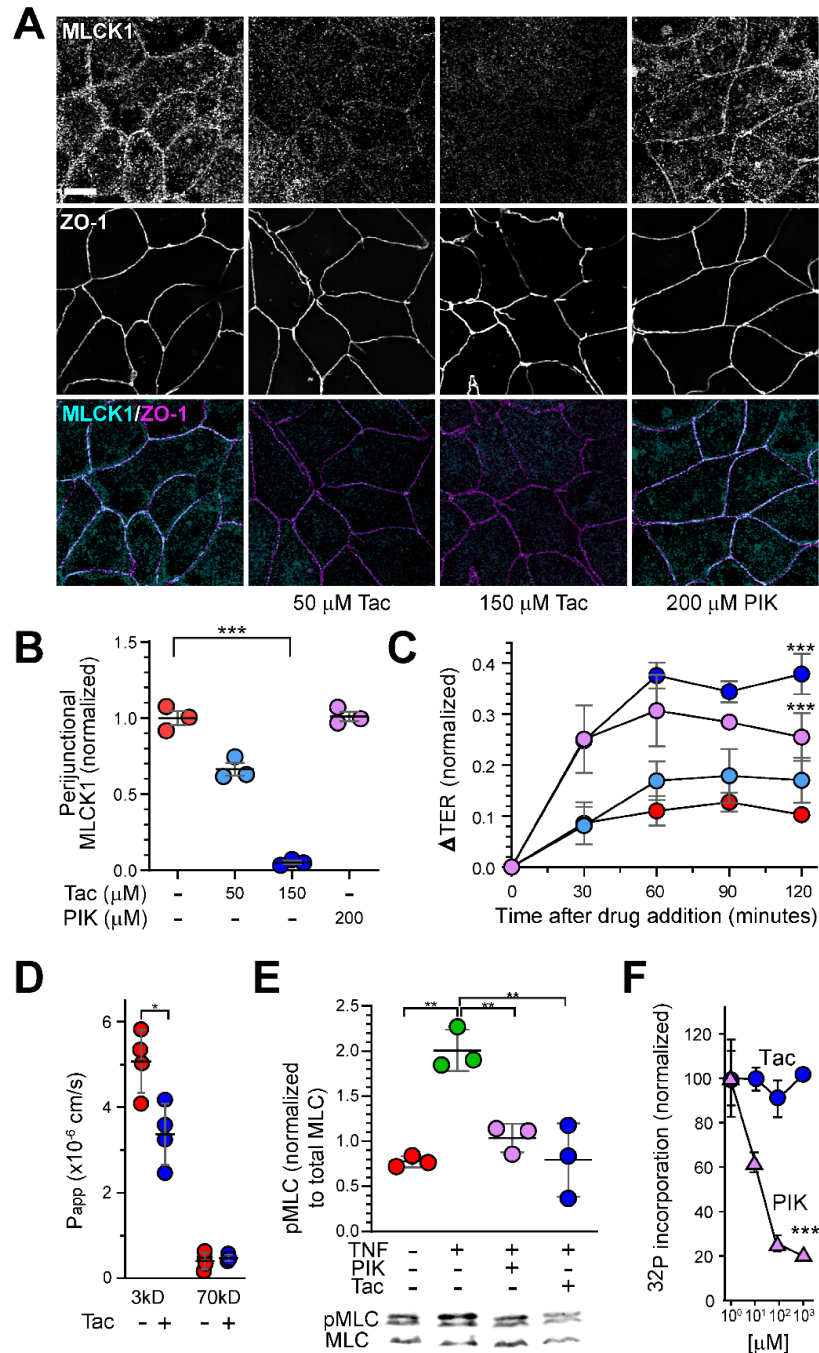


Figure S1. Tacrolimus displaces MLCK1 and increases barrier function in a dose-dependent manner. A, B. Vehicle, 50 μM tacrolimus, 150 μM tacrolimus, or 200 μM PIK were added to monolayers apically. Samples were fixed after 2 h and

immunostained for MLCK1 (cyan) and ZO-1 (magenta). Quantitative analysis shows that 150 μ M tacrolimus displaces perijunctional MLCK1. Bar = 10 μ m. **C.** Caco2_{BBE} monolayers were treated with vehicle (red), 50 μ M tacrolimus (light blue), 150 μ M tacrolimus (dark blue), or 200 μ M PIK (purple). $n = 3$ independent samples in this experiment, which is representative of >3 experiments. *** $P < 0.001$; ANOVA. **D.** Caco2_{BBE} monolayers were treated with vehicle (red) or 150 μ M tacrolimus (dark blue) for 2 h. $n = 3$ independent samples in this representative experiment. * $P < 0.05$; Student's t-test. **E.** Representative western blots and quantitative analysis of MLC phosphorylation in Caco2_{BBE} monolayers treated with TNF (1ng/ml) for 4 h. Tacrolimus (150 μ M, blue) or PIK (200 μ M, purple) was added 2 h before harvest. TNF induced MLC phosphorylation which was blocked by both PIK and tacrolimus. $n = 3$ independent samples in this experiment, which is representative of >3 experiments. ** $P < 0.01$; ANOVA. **F.** An in vitro MLC kinase assay was performed using recombinant MLC, Caco-2 cell lysates as a source of MLCK, and ³²P-ATP. Enzymatic activity was inhibited by PIK but not tacrolimus. $n = 3$ independent samples in this experiment, which is representative of >3 experiments. *** $P < 0.001$; Student's t-test.

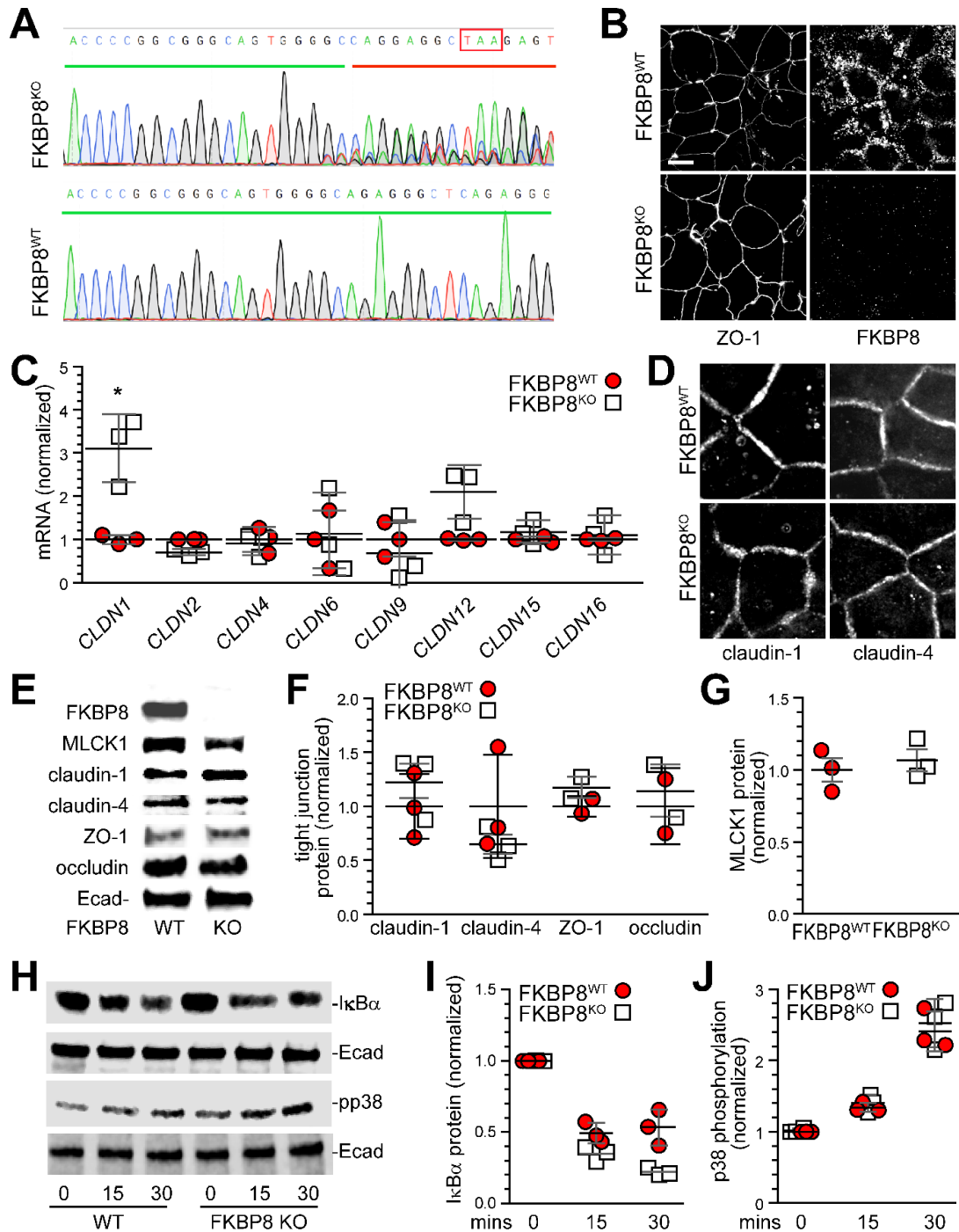


Figure S2. FKBP8 knockout does not affect tight junction protein expression or TNF signaling. **A.** Sequence analysis of KO genomic DNA showing generation of a stop codon within the gRNA target site. WT sequence is shown for reference. **B.** Immunostaining for FKBP8 and ZO-1 confirms absence of FKBP8 expression in KO Caco-2 cells. **C.** qRT-PCR comparing claudin expression in *FKBP8*^{KO} (open squares) and WT (red circles) Caco-2 cells. *n* = 3 independent samples in this representative experiment. **P* < 0.05; Student's t-test. **D.** Representative micrograph showing similar claudin-1 and claudin4 expression in WT and *FKBP8*^{KO} Caco-2 cells despite increased *CLDN1* mRNA in *FKBP8*^{KO}. **E, F, G.** Representative western blots and quantitative densitometry of WT (red circles) and *FKBP8*^{KO} (open squares) Caco-2 cells. Claudin-1 protein expression was similar in WT and *FKBP8*^{KO} Caco-2. MLCK1 expression was also unaffected by FKBP8 KO. *n* = 3 independent samples in this representative experiment. **H, I, J.** Primed *FKBP8*^{KO} (open squares) and WT (red circles) monolayers were treated with TNF (1 ng/ml) and harvested for western blot and quantitative densitometry after 15 and 30 mins. IκBα degradation content and increased p38 MAPK phosphorylation (pp38) demonstrate similar activation of TNF signaling in both KO and WT Caco-2. *n* = 3 independent samples in this representative experiment.

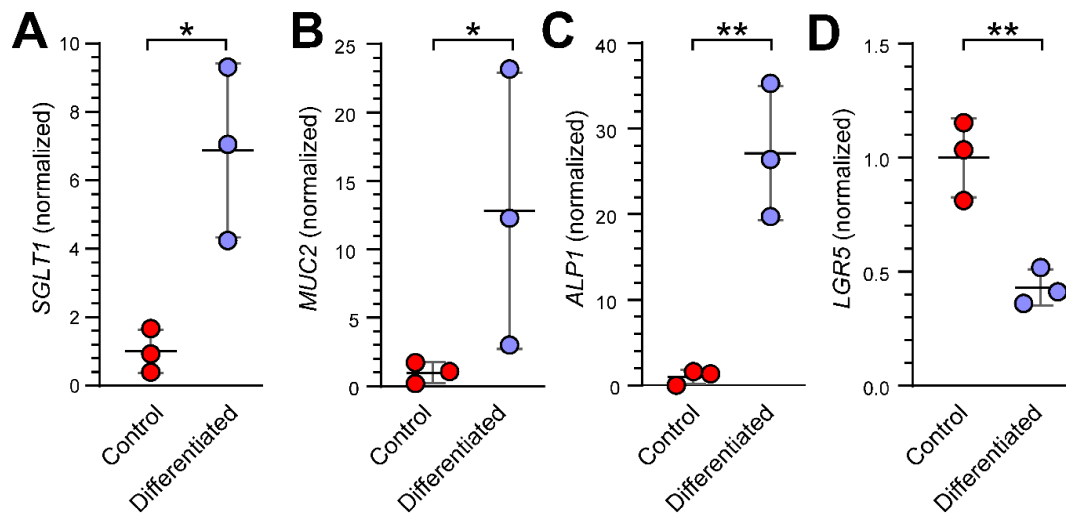


Figure S3. Differentiation of human organoids.

Human organoids were grown in growth medium for 14 days (red circles) or growth medium for 2 days and then transferred to differentiation medium for 12 days. qPCR was performed to detect mRNA expression of *SGLT1*, *MUC2*, *ALP1*, and *LGR5*, as shown. $n = 3$ independent samples in this representative experiment. *, $P < 0.05$; **, $P < 0.01$; Student's t-test.

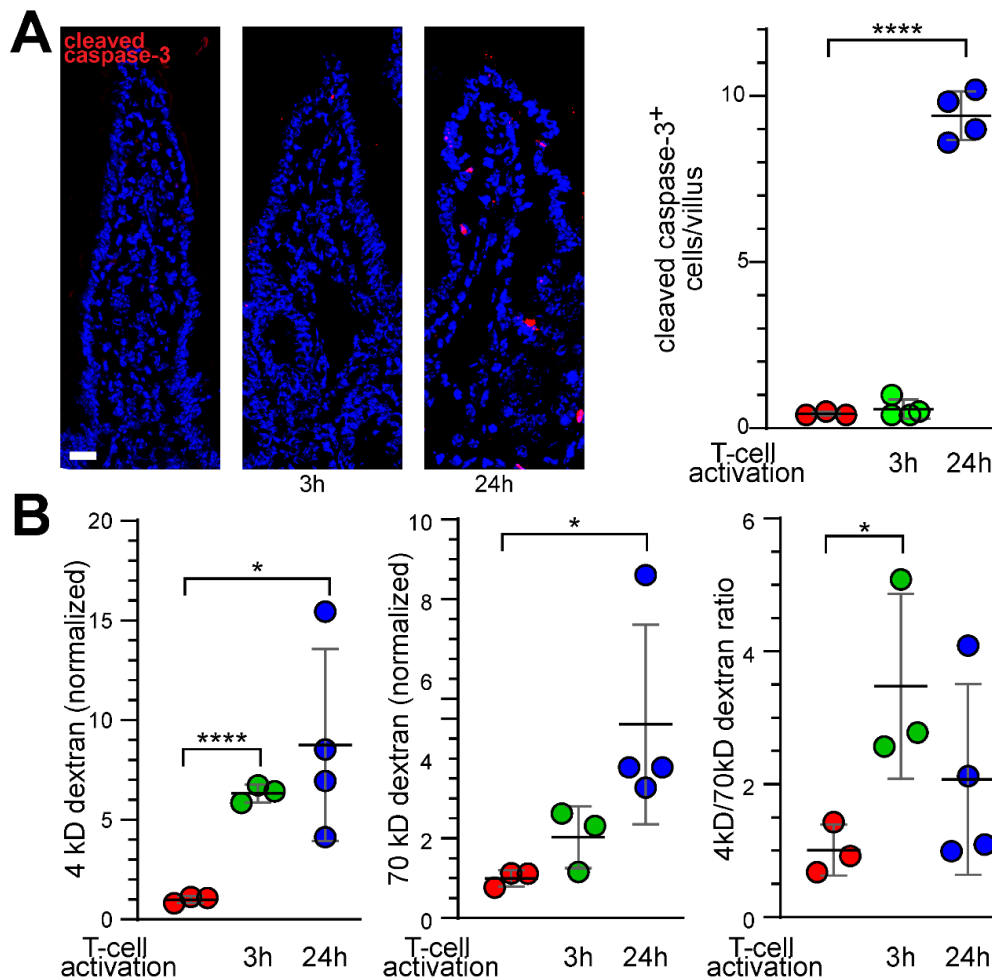


Figure S4. Anti-CD3 induces apoptosis after 24 h but not after 3 h. **A.** Mice were injected with saline or 200 μ g anti-CD3 (clone 2C11) and sacrificed 3 h or 24 h later. Immunostains show cleaved caspase-3 (red) and nuclei (blue) in jejunum. **B.** Mice were gavaged with 4kD FITC- dextran and 70kD rhodamine-dextran 3 h before sacrifice. Serum dextran concentrations were determined and normalized to the mice that received saline. Only 4kD dextran permeability increased at 3 h, indicating tight junction leak pathway regulation. In contrast, 70kD dextran permeability, a marker of damage, as well as 4kD dextran permeabilities were increased at 24 h. The ratio of 4kD/70kD dextran indicates leak pathway regulation (without damage) and damage at 3 h and 24 h, respectively. $n = 3 - 4$. *, $P < 0.05$; ****, $P < 0.0001$; Student's t-test.

Supplemental Materials and Methods

Cell culture

Caco-2_{BBE} monolayers (clone 5E6L) were cultured and plated on Transwells (3413, Corning) as previously described¹ and used for experiments between 17 and 21 days post-confluence. Cells were transfected with gRNA (5'-CCGGCGGGCAGUGGGGC-3') and Cas9 (Synthego) using Lipofectamine Cas9 Plus (Invitrogen) to create *FKPB*^{KO} lines. Results were similar in two independent clones. Plasmids were stably co-transfected with pSuper PiggyBac-transposase (System Biosciences).

Doxycycline (50 ng/ml) was added 24 h previous to study. For experiments in which some monolayers were treated with TNF, monolayers were primed with interferon- γ (R&D Systems) at 2 ng/ml for 18 h before addition of TNF (R&D Systems) at 1 ng/ml. Cytokines were added only to the basolateral media. Tacrolimus (FK506, Sigma) was prepared as a stock in DMSO and, after dilution, added to the apical media only. Dr-PIK^{2,3} was prepared in media and added apically. TER was measured using an EVOM3 (World Precision Instruments) or voltage clamp (Physiologic Instruments) as described.⁴

Human organoid culture

Duodenal biopsies were obtained from de-identified endoscopic biopsies. Only macroscopically normal-appearing tissue was used from patients without a known gastrointestinal diagnosis. After a brief wash with pre-warmed DMEM/F12, biopsies were digested in 2 mg/ml of collagenase type I reconstituted in HBSS for 40 minutes at 37°C. Samples were then agitated by pipetting followed by centrifugation at 500 x g for 5 minutes at 4°C. The supernatant was then removed, and crypts resuspended in 200-300 μ l of Matrigel, with 50 μ l being plated onto 4-6 wells of a 24-well plate and polymerized at 37°C. Isolated crypts in Matrigel were grown in specific growth media (GM) based on the tissue of origin. The resulting organoids were passaged every 6-8 days as needed, with media changes occurring every two days. To passage, Matrigel was mechanically dissociated from the well and resuspended in 500 μ l of Cell Recovery solution for 40-60 minutes at 4°C. To aid in separating the Matrigel and enteroids, the tubes are gently inverted and then centrifuged at 500 x g for 5 minutes at 4°C. The supernatant was then removed, and organoids resuspended in Matrigel, followed by mechanical disruption via a bent-tipped pipette. Organoids were passaged at a 1:2 dilution, with 50 μ l per well of a 24-well plate. After plating, the organoids were incubated at 37°C for 10 minutes to allow the Matrigel to set. Once complete, 500 μ l of growth medium (GM) was added to each well. GM composition⁵ was: L-WRN conditioned media (50% v/v), DMEM/F12 (45% v/v), Glutamax (1% v/v), N-2 Supplement (1% v/v), B-27 Supplement (1% v/v), HEPES (10mM), primocin (100 μ g/mL), normocin (100 μ g/mL), A83-01 (500nM), N-acetyl-cysteine (500 μ M), recombinant murine EGF (50ng/mL), Human [Leu15] gastrin I (50nM), nicotinamide (10mM), and SB202190 (10 μ M).⁵

For differentiation, organoids were passaged and grown in GM for two days, to allow for ISC expansion, after which the organoids were transitioned to tissue-specific differentiation medium (DM). DM composition was the same as GM except that nicotinamide and SB202190 were omitted and replaced by DAPT (20 μ M), betacellulin (20ng/mL), tubastatin-A (10 μ M), PF06260933 (6 μ M), and tranlycypromine (1.5 μ M).⁵ Media was changed every two days, with tubastatin A being removed after the second day of differentiation. Enteroids were released using cell

recovery solution at 4°C before further analysis.

Differentiated organoids were treated with vehicle or TNF (1 ng/ml) for 4 h, after which vehicle, tacrolimus (150 µM), or PIK (200 µM) were added for 2h before fixation.

Immunostaining

Formalin-fixed, paraffin-embedded mouse tissues were assembled into tissue microarrays before staining. After deparaffinization, 5 µm sections were rehydrated, and epitopes were unmasked by heating in a pressure cooker in 0.01 M citrate buffer, pH 6.0 (Dako) for 15 min. After cooling, sections were incubated in bleaching buffer (24 mM NaOH, 9% H₂O₂) under bright broad-spectrum illumination for 1 h at room temperature. After one 10 min wash in PBS, sections were incubated with blocking buffer (Dako) for 20 min. Primary antibodies prepared in antibody diluent (Dako) were added overnight at room temperature. After three 10 min, incubations with wash buffer (Dako), secondary antibodies prepared in antibody diluent were added for 1 h. After washing and rinsing once in the water, sections were mounted using Prolong Diamond.

For analysis of occludin internalization in tissue, 5 µm sections of snap-frozen, OCT embedded tissue were cut and fixed in -20°C methanol. After 3 washes with PBS, PBS⁺/BS³ solution⁶ was added and the slides were incubated for 30 min at room temperature. The slides were incubated in blocking buffer (Dako) and primary antibodies prepared in antibody diluent (Dako) were added. After washing, secondary antibodies were applied. Sections were then washed and mounted using Prolong Diamond.

Cell monolayers were fixed in -20°C methanol and stained as for frozen tissue sections. Membranes were then excised from Transwell supports and mounted using SlowFade Diamond.

Proximity ligase assay

Methanol-fixed Caco-2_{BBE} monolayers, paraformaldehyde-fixed organoids, or deparaffinized, antigen-retrieved, biopsy tissue sections were blocked, incubated with rabbit anti-MLCK1 and mouse anti-FKBP8 antibodies overnight at 4°C. After washing, oligonucleotide-linked secondary antibodies were applied for 1 h at 37 °C, washed, and incubated with polymerase and nucleotide for 2 h at 37°C. Samples were then labeled with rat anti-ZO-1 and Alexa647-conjugated donkey anti-rat antibodies, washed, and mounted for imaging.

Imaging and post-acquisition analysis

Fluorescent-stained tissue sections were imaged using an Axioplan 2 microscope (Zeiss) with 20x NA 0.8 Plan-Apochromat and 100x NA 1.4 Plan-Neofluar objectives, and a Coolsnap HQ (Photometrics) camera controlled by MetaMorph 7 (Molecular Devices). Stained monolayers were imaged using a DM6000 microscope (Leica) with CSU-X1 spinning disk (Yokogawa), 20x NA 0.7 HC PLAN APO and 100x NA 1.4 HC PLAN APO CS2 objectives, and a Zyla 4.2 Plus sCMOS camera (Andor) controlled by

MetaMorph. Post-acquisition processing and analyses used MetaMorph 7, Autoquant X3 (MediaCybernetics), Image J/FIJI, and Imaris 9.7 (Bitplane). The perijunctional fraction of MLCK1 was quantified by creating a mask using ZO-1 to define the perijunctional actomyosin ring. MLCK1 fluorescent signal overlapping with this mask is expressed as a fraction of MLCK1 signal within the entire area of the mask, i.e., the entire cell.⁷ Masks defined by ZO-1 staining were used in the same manner to quantify myosin light chain phosphorylation at the perijunctional actomyosin ring. Numbers of occludin vesicles were quantified using ImageJ to identify appropriately sized vesicles, i.e., spots, within the cytoplasm.

RNA isolation and quantitative RT-PCR

RNA was purified from epithelial cells or intestinal sections lysed in RLT buffer using RNeasy mini-columns (Qiagen). RNA quality was evaluated using the RNA 6000 Nano Kit and 2100 Bioanalyzer (Agilent Technologies). After digestion with RNase-free DNase, 1 µg of RNA was reverse transcribed and analyzed by qRT-PCR using SsoFast Universal SYBR (Bio-Rad) and a CFX96 thermocycler (Bio-Rad).

In vivo intestinal perfusion and permeability analysis

In vivo perfusions were performed as described previously.⁸ C57BL/6J female mice (8-12 week-old) were fasted prior to each experiment. Anesthesia was induced after treatment with anti-CD3 (200 µg, clone 2C11, Bio X Cell) or vehicle with ketamine (75 mg/kg, intraperitoneal injection; Fort Dodge Animal Health) and xylazine (25 mg/kg, intraperitoneal injection; Lloyd Laboratories). This was followed by perfusion of 5 ml solution (50 mM NaCl, 5 mM HEPES, 2.5 mM KCl, 20 mM glucose, 0.2 mg/ml 4 kD-fluorescein dextran, 0.05 mg/ml 70 kD-rhodamine-dextran, pH 7.4) with vehicle or or 600 µM tacrolimus in a recirculating manner at 1 ml/min for 3h, beginning 1 h after anti-CD3 injection. Blood was collected for analysis as described.⁹

Intestinal permeability analysis in intact mice

Mice were injected with anti-CD3 or vehicle as described for intestinal perfusion assays. Those that received vehicle and one group of mice that received anti-CD3 were immediately gavaged with 4 kD-fluorescein dextran and 70 kD-rhodamine-dextran, exactly as described.⁹ Serum was collected 3 h later and dextran content was analyzed. A second group of mice were gavaged with fluorescent dextrans 21 h after anti-CD3 injection. Serum was collected from these mice 3 h later, i.e., 24 h after T cell activation.

Microscale thermophoresis

Recombinant proteins were expressed in Rosetta2 (DE3)pLysS bacteria (Novagen) and purified on GST or IMAC columns (Bio-Rad) using an AktaPure (GE) system. HRV protease (Millipore) was used to remove GST tags. For microscale thermophoresis, His-tagged MLCK IgCAM1-4 or IgCAM3 were labeled using MonolithNT His-Tag Labeling

Kit (NanoTemper). Microscale thermophoresis was performed using a Monolith NT.115 (NanoTemper). Data were analyzed by MO Affinity Analysis software.

ELISA

ELISA assays of mucosal lysates were performed using Quansys multiplex plates according to the manufacturer's instructions.

In vitro MLC kinase assay

Confluent Caco-2_{BBE} monolayers expressing MLCK1 and MLCK2 were used as the source of MLC kinase. After dilution in kinase reaction buffer (20 mM 3-morpholinopropane-1-sulfonic acid, pH 7.4, 2 mM MgCl₂, 0.25 mM CaCl₂, and 0.2 μM calmodulin), tacrolimus or PIK were added. The reaction was initiated by the addition of γ³²P-ATP (ICN) and 5 μM recombinant MLC and incubating at 30°C for 15 min. MLC phosphorylation was determined by autoradiography after SDS-PAGE.

Statistical analysis

All data are presented as mean ± SD and are representative of at least 3 independent experiments. In addition, each in vitro experiment evaluated Transwells within at least 3 separate wells. Statistical significance was determined by 2-tailed Student's t-test or ANOVA with Bonferroni's correction, as indicated in the figure legends. Results with *P* less than 0.05 were considered significant. In all figures, *, *P* < 0.05; **, *P* < 0.01; ***, *P* < 0.001; ****, *P* < 0.0001.

Primers

Gene	Forward primer (5'-3')	Reverse primer (5'-3')
Human		
<i>CDH1</i>	TGCCAGAAAATGAAAAAGG	GTGTATGTGGCAATGCGTTC
<i>CLDN 2</i>	GAGGGATTAGAGGTGTTCAAG G	CTAGGATGTAGCCCACAAGTTG
<i>CLDN1</i>	TTGGGCTTCATTCTCGCCTT	GTCGCCGGCATAGGAGTAAA
<i>CLDN1</i>	GGGATTTCGCACCTGTGATGA	GCTCGAGTTACCACCAGCTT
<i>CLDN12</i>	CAGTTTGCCCTACCCCTCAG	CAGTTTGATGTTGGGCACCG
<i>CLDN15</i>	TCTGGTTTAGCTGTGCCACC	CTATGCCTAGCAAGAGGCCG
<i>CLDN4</i>	CACAGACAAGCCTTACTCCG	CTAGGATGTAGCCCACAAGTTG
<i>CLDN6</i>	ATGCAGTGCAAGGTGTACGA	CCAGCAAGGTAGACCAGCAA
<i>CLDN9</i>	ATGCAGTGCAAGGTGTACGA	TACTGCGGCACCTGTGATG
<i>ALP1</i>	GTATGTGTGGAACCGCACTG	CTGGTAAGCCACACCCTCAT
<i>SGLT1</i>	TGCTGGTGGGGTCTTTAATC	GGATCTCGGAAGATGTGGAA
<i>MUC2</i>	GGGCAGCTAACATCTCTTGC	AGTTGAGGCAGAAGGCCATA
<i>MLCK1/2</i>	TCTGAGAAGAACGGCATG	ACTTCAGGGGGTGGATTC
<i>LGR5</i>	CTCTTCCTCAAACCGTCTGC	GATCGGAGGCTAAGCAACTG
Mouse		
<i>Cdh1</i>	TCCTTGTTTCGGCTATGTGTC	GGCATGCACCTAAGAATCAG
<i>Ifng</i>	TCAAGTGGCATAGATGTGGAAGAA	TGGCTCTGCAGGATTTTCATG
<i>Il17</i>	TTCAGGGTCGAGAAGATGCT	AAACGTGGGGGTTTCTTAGG
<i>Il1b</i>	GAGTGTGGATCCCAAGCAAT	TACCAGTTGGGGAACCTCTGC
<i>Il6</i>	CCGGAGAGGAGACTTCACAG	TCCACGATTTCCAGAGAAC
<i>Kc</i>	TGTTGTGCGAAAAGAAGTGC	TACAAACACAGCCTCCCACA
<i>mMyk</i>	GCGTGATCAGCCTGTTCTTTCTAA	GCCCCATCTGCCCTTCTTTGACC
<i>Tnfsf2</i>	AGCCCCAGTCTGTATCCTT	GGTCACTGTCCCAGCATCTT

Antibodies

Protein	Species	Source	RRID	Concentration
CD3	Rabbit	Abcam ab16669	AB_443425	1 µg/ml (IF)
E-cadherin	Mouse	Abcam ab76055	AB_1310159	1 µg/ml (IF)
NaKATPase	Mouse	Abcam ab7671	AB_306023	5 µg/ml (IF)
OCLN (mouse)	Rat	Clone 6B8A3	AB_2819194	1 µg/ml (IF)
OCLN (human)	Rat	Clone 5E5A6	AB_2819196	1 µg/ml (IF)
ZO-1 (human)	Rat	Clone 6B6E4	AB_2783858	1 µg/ml (IF)
ZO-1 (mouse)	Rat	Clone R40.76	AB_2783859	1 µg/ml (IF) 0.1 µg/ml (WB)
MLCK1	Rabbit	pab0674	AB_2894908	5 µg/ml (IF) 0.5 µg/ml (WB)
MLCK1	Rat	pab0675	AB_2909525	5 µg/ml (PLA)
FKBP8	Mouse	R&D system MAB3580	AB_2262675	1:100 (IF) 1:500 (WB)
IκBα	Mouse	Cell Signaling 4814	AB_390781	1:100 (WB)
phospho-p38	Mouse	Cell Signaling 9216	AB_331296	1:100 (WB)
phospho-MLC	Rabbit	Cell signaling 3671	AB_330248	1:100 (WB)
Cleaved-caspases3	Rabbit	Cell Signaling 9664	AB_2070042	1 µg/ml (IF)
AF488-anti-rabbit IgG F(ab') ₂	Donkey	Jackson ImmunoResearch 711-545-152	AB_2313584	3 µg/ml (IF)

AF594-anti-mouse IgG F(ab') ₂	Donkey	Jackson ImmunoResearch 715-585-150	AB_2340854	3 µg/ml (IF)
AF647-anti-rat IgG F(ab') ₂	Donkey	Jackson ImmunoResearch 712-605-153	AB_2340694	3 µg/ml (IF)
IRDye 800CW-anti-rat IgG	Goat	LI-COR Biosciences 925-32219	AB_2721932	0.1 µg/ml (WB)
IRDye 800CW-anti-rabbit IgG	Goat	LI-COR Biosciences 926-32211	AB_621843	0.1 µg/ml (WB)
IRDye 680RD anti-mouse IgG	Goat	LI-COR Biosciences 926-68070	AB_10956588	0.1 µg/ml (WB)

Plasmids

All construct were validated by sequencing.

Name	Plasmid ID	Use
pGEX6P1-FKBP8	p0867	Microscale thermophoresis
pGEX6P1-FKBP8 ^{ΔTM}	p0985	Microscale thermophoresis
pGEX6P1-FKBP8 ^{PPi}	p0987	Microscale thermophoresis
pET21-MLCK1(IgCAM1-4)-His	p1252	Microscale thermophoresis
pET21-MLCK1(IgCAM3)-His	p1415	Microscale thermophoresis
pGEX6P1-MLCK1(IgCAM3)	p0670	Microscale thermophoresis
pET34b(+)-MLC	p0067	In vitro kinase assay
pPBH-TREtight-mCherry-FKBP8	p0769	Caco-2 expression
pPBH-TREtight-FKBP8 ^{PPi}	p1339	Caco-2 expression
pPBH-TRE tight-FKBP8 ^{ΔPPi}	p1340	Caco-2 expression
pSPB-transposase (System Biosciences)	PB200A-1	Caco-2 transfection
pGBKT7-MLCK1(IgCAM2-5)	p0159	Yeast-2-hybrid
pGBKT7-MLCK2(IgCAM2-5)	p0161	Yeast-2-hybrid
pGADT7-MLCK1(IgCAM1-4)	p1161	Yeast-2-hybrid
pGADT7-MLCK2(IgCAM1-4)	p1162	Yeast-2-hybrid
pGBKT7BD.FKBP8	p1165	Yeast-2-hybrid
pGBKT7BD-FKBP8(ΔERD)	p1166	Yeast-2-hybrid
pGBKT7BD-FKBP8(ΔPPI)	p1167	Yeast-2-hybrid
pGBKT7BD-FKBP8(ΔTPR1)	p1168	Yeast-2-hybrid
pGBKT7BD-FKBP8(ΔTM)	p1170	Yeast-2-hybrid

Supplemental references

1. Pongkorpsakol P, Turner JR, Zuo L. Culture of intestinal epithelial cell monolayers and their use in multiplex macromolecular permeability assays for in vitro analysis of tight junction size selectivity. *Curr Protoc Immunol* 2020; 131:e112.
2. Zolotarevsky Y, Hecht G, Koutsouris A, et al. A membrane-permeant peptide that inhibits mlc kinase restores barrier function in in vitro models of intestinal disease. *Gastroenterology* 2002; 123:163-72.
3. Owens SE, Graham WV, Siccardi D, et al. A strategy to identify stable membrane-permeant peptide inhibitors of myosin light chain kinase. *Pharm Res* 2005; 22:703-9.
4. Shashikanth N, Rizzo HE, Pongkorpsakol P, et al. Electrophysiologic analysis of tight junction size and charge selectivity. *Curr Protoc* 2021; 1:e143.
5. Zeve D, Stas E, de Sousa Casal J, et al. Robust differentiation of human enteroendocrine cells from intestinal stem cells. *Nat Commun* 2022; 13:261.
6. Shen L, Turner JR. Actin depolymerization disrupts tight junctions via caveolae-mediated endocytosis. *Mol Biol Cell* 2005; 16:3919-36.
7. Graham WV, He W, Marchiando AM, et al. Intracellular mlck1 diversion reverses barrier loss to restore mucosal homeostasis. *Nat Med* 2019; 25:690-700.
8. Clayburgh DR, Barrett TA, Tang Y, et al. Epithelial myosin light chain kinase-dependent barrier dysfunction mediates t cell activation-induced diarrhea in vivo. *J Clin Invest* 2005; 115:2702-15.
9. Chanez-Paredes SD, Abtahi S, Kuo WT, et al. Differentiating between tight junction-dependent and tight junction-independent intestinal barrier loss in vivo. *Methods Mol Biol* 2021; 2367:249-271.